THESIS REPORT ON

Synthesis and characterization of manganese zinc ferrite

Submitted by

ARVIND KUMAR

Student of **M.Tech.**

Materials Science and metallurgical Engineering

Thapar University, Patiala

Work done at

NATIONAL PHYSICAL LABORATORY

Dr. K. S. KRISHNAN MARG

NEW DELHI-110012

DEDICATED TO MY

FAMILY

DECLARATION

I hereby declare that the report entitled **"Synthesis and characterization of Magnese Zinc Ferrite"** is an authentic record of my own work carried out as requirements for the award of degree of M.Tech. (Materials Science and Metallurgical Engineering) at Thapar University, Patiala, under the guidance of Dr. R.P.Pant (Scientist F, NPL, New Delhi) and Dr. Puneet Sharma (Assistant Professor, MSE) during January to July 2010.

Date: 13/7/10

(Arvind Kumar)

Roll No. - 600802027

It is certified that the above statement made by the candidate is correct to best of my knowledge and belief.

15/7/10

Dr. R.P.Pant
Scientist F
Head of EPR Spectroscopy Section
NPL, New Delhi

Dr. Puneet Sharma
Assistant Professor
Thapar University, Patiala

Dr. O.P.Pandey
Professor & Head, MSE,
Thapar University, Patiala

Dr. R.K. Sharma 16/7/10
Dean of Academic Affairs
Thapar University, Patiala

CERTIFICATE

This is to Certified that **Mr. ARVIND KUMAR**, student of M. Tech. Materials Science and Engineering from Thapar University, Patiala, Punjab, has completed the dissertation entitled ***"Synthesis and Characterization of manganese zinc ferrite"*** under my supervision at National Physical Laboratory (NPL) in E.P.R. spectroscopy section.

The above said project has been carried out during the period from 20th January, 2010 to 20th July, 2010.

18/7/2010

Dr. R. P. Pant Scientist 'F'

डा० आर० पी० पंत / Dr. R. P. PANT
वैज्ञानिक / Scientist
Head EPR Section
राष्ट्रीय भौतिक प्रयोगशाला / NPL

Head of EPR Spectroscopy Section

National physical Laboratory,

Dr. K. S. Krishnan Marg

New Delhi -110012

Acknowledgements

First of all, I wish to thank **Professor R. C. Budhani**, Director, NPL, for allowing me to carry out this project as a part of my internship program-II at his esteemed research organization.

I am extremely indebted to **Dr. R. P. Pant**, Scientist-F, without whose guidance and support, I couldn't have completed this work. He was instrumental in assigning me this work; he provided all the required resources and ensured by all means that I come up with valid results.

I owe my sincere thanks to **Miss Manju Arora**, for his critical approach towards my work, Scientist, who monitored us regularly, encouraged us throughout the work and showed us the proper way to channelise our efforts in right direction.

Finally, I am also thankful to **Mr. Ashok Kumar, Mr. Sandeep Kumar, Mr. Ajay Sankar** and **Mr. Mahesh chand,** JRFs, Deptt. Of EPR Spectroscopy section, who, whenever asked for, extended their kind help to me.

Finally my deepest appreciation goes to my respected parents **Shri Rishipal singh** and **Smt. Rajeshwari,** who encouraged me to complete my higher studies. My special thanks to my brothers **Amit kumar singh** , **Anil kumar singh** and sister in law **Mrs. Arti singh** and my naughty

friends **Pankaj baluni, Hirdesh pharasi, Sambhu and Sunil Thapa, Sunil Rawat** for their encouragement and help in all possible ways during the period of my project work.

My wholehearted thanks, to my classmates and friends, **Anil kumar, Ravinder Kumar, N.P.Misra, Lovekush , Gaurav Singla, Alok Misra, Arvind Chauhan and Vasu** for their co-operation and blessings which gave me a super natural power to face the problems and solve them with confidence

ARVIND KUMAR

National physical Laboratory

Dr. K. S. Krishnan Marg

New Delhi -110012

Contents

Abstract

This report intends to elicit information in relation to a research-based project carried out at National Physical Laboratory, New Delhi. As the work has been pursued in two broadly different areas so the report has been divided into two parts, Part-A on the Magnetic Materials and, Ferrites materials and their application in ferrofluid and Part-B on the Synthesis and Characterization of Manganese zinc Ferrite .

The report begins with a brief section on the NPL - its history, objectives, research aras, technologies it has developed over the years, etc. Thereafter, a detailed description of the Magnetic Materials, Ferrites and spinel ferrite has been included in Part-A, covering its structure, principle of operation, and its areas of applications so as to make a smooth transition to higher concepts later on. Henceforth, the details of the theoretical and experimental work have been incorporated.

In Part-B, the details of the work on synthesis and characterization of manganese zinc Ferrite by co-precipitation route has been included. After furnishing details of the experimental procedure and obtained results, a brief account of the instruments has been provided to make this project more helpful for the readers.

I am confident that this report will be of immense value and will do some value addition to the knowledge of its readers.

About NPL

The National Physical Laboratory is the premier research laboratory in India in the field of physical sciences. Established in 1947, it is one of the oldest laboratories of the Council of Scientific and Industrial Research. It has developed core competencies in standards, apex level calibration, engineering materials, electronic materials, materials characterization, radio and space physics, global change and environmental studies, low temperature physics, and instrumentation. Its main activities are:

- Research and development
- Consultancy
- Sponsored and contract research
- Calibration and testing

1.1. RESEARCH AREAS

- Measurement Standards
- Physico-Mechanical Standards
- Electric & Electric Standards
- Engineering Materials
- Electronic Materials
- Materials Characterization
- Radio & Atmospheric Sciences
- Superconductivity & Cryogenics

1.2. CALIBRATION & TESTING

Center for Calibration & Testing **(**CFCT) has been established to promote Calibration & Testing Services of the laboratory. It acts as an interface between all the calibrating & testing groups of the NPL and nearly 3500 customers from industries, various laboratories and government organizations from all over the country and abroad. We understand the requirements of the customer and thus stand for the customer satisfaction to the best of our endeavor.

Your satisfaction is our pleasure.

1.2.1. Fabrication

Besides calibration and testing facilities provided to the customers for maintaining the national traceability chain of measurement, NPL has developed the know-how for fabrication of some items to be used by the customers. The fabricated items are not available of the shelf as the fabrication is done as per customer's demand and specifications. The areas and items of fabrication are as follows:

- **Thin Film Coating**
- **Temperature & Humidity**

1.2.2. Technologies Developed

- Miniature Teleclock
- Piezoelectric Accelerometer
- Carbon Composite Half rings for Orthopaedic Applications
- Temperature Calibration Bath
- Magical Heat PAD/PACK (Reusable)
- Basic Sodar Operating in Monostatic/Doppler Mode
- Long Afterglow Phosphor
- Blood Glucose Digital Analyzer
- Force Transducer/ Load Cells
- Impregnating-Grade Coal Tar Pitch
- Porous Conducting Caron Paper
- Dead Weight Piston Gauge Pressure standard upto 80 Mpa

1.2.3. Quality Policy

- To establish, maintain and upgrade the national standards of measurement compatible to international standards through continuous research and development.
- To provide apex level calibration and dissemination of standards for maintaining traceability of measurement standards following quality system as per ISO 17025 consciously and effectively.

1.2.4. Objectives

- To provide calibration and testing within specified time and to the satisfaction of the customers.
- To familiarize all personnel concerned in calibration and testing with quality system documentation and implementation of policies and procedures.

1.3. CORE COMPETENCIES DEVELOPED AT NPL	
Standards	Time & frequency; quantum metrology; optical measurements; pressure & vacuum; and certified reference materials
Apex level calibration	Dimensional metrology; force & hardness; optical radiation; mass, AC &LF power & energy
Engineering materials	Metals, alloys & components for aerospace applications; carbon fibers & composites; super hard materials; polymer & soft materials; liquid crystals and biosensors
Electronic materials	Luminescent materials; photovoltaic materials and devices; thin films; special ceramics; crystal growth; and elecrochromic devices

Materials characterization	Composition and trace impurity analysis; structural characterization & evacuation of perfection of epitaxial films, bulk crystals and interfaces
Radio and space physics	Radio communication & media characterization; space physics
Global change & environmental	Atmospheric environment monitoring; and global change studies
Low temperature physics	Superconductivity; SQUIDS; cryogenics; and superconducting magnets
Instrumentation	X-ray diffraction; pressure metrology; X-ray radiography; biosensors; particle size analyzers; and rocket and satellite payloads

Chapter 1

1.1 INTRODUCTION TO MAGNETIC MATERIALS

The term magnetism is derived from Magnesia, the name of a region in Asia Minor where lodestone, a naturally magnetic iron ore, was found in ancient times. Iron is not the only material that is easily magnetized when placed in a magnetic field; others include nickel and cobalt. Carbon steel was long the material commonly used for permanent magnets, but more recently other materials have been developed that are much more efficient as permanent magnets, including certain ferroceramics and Alnico, an alloy containing iron, aluminum, nickel, cobalt, and copper. Magnetic materials can be classified based on their properties in particular permeability. Major types of magnetic materials fall into categories of diamagnetism, paramagnetism and ferromagnetism.

1.2 TYPES OF MAGNETISM

1.2.1 DIAMAGNETISM

Diamagnetism is a form of magnetism which is exhibited by a substance in the presence of an externally applied magnetic field [1]. It is the result of changes in the orbital motion of electrons. The applied magnetic field creates a magnetic force on a moving electron which is given by **F = q (v x B)**. This magnetic force changes the centripetal force on the electron, causing it to either speed up or slow down in its orbital motion. This changed electron speed modifies the magnetic

moment of the orbital in a direction opposing the external field. Consider two electron orbitals: one rotating clockwise and the other counterclockwise. An external magnetic field into the page will make the centripetal force on an electron rotating clockwise increase, which increases its moment out of the page. That field would make the centripetal force on an electron rotating counterclockwise decrease, decreasing its moment into the page. Both changes oppose the external magnetic field into the page. However, the induced magnetic moment is very small in most everyday materials.

1.2.2 PARAMAGNETISM

Paramagnetism is a form of magnetism, which occurs only in the presence of an externally applied magnetic field [2]. Paramagnetic materials are attracted to magnetic fields; hence have a relative magnetic permeability greater than one, while the positive magnetic susceptibility. However, unlike ferromagnets, which are also attracted to magnetic fields, paramagnets do not retain any magnetization in the absence of an externally applied magnetic field. Constituent atoms of paramagnetic materials have permanent magnetic dipoles moments, even in the absence of an applied field. This generally occurs due to the presence of unpaired electrons in the atomic orbital. In pure paramagnetism, the dipoles are randomly oriented in the absence of an external field and do not interact with one another, resulting in zero net magnetic moment.

When a magnetic field is applied, the dipole gets aligned along the applied field. In the classical description, this alignment can be understood to occur due to a torque being provided on the magnetic moments by an applied field, which tries to align the dipoles parallel to the applied field. However, the truer origins of the alignment can only be understood via the quantum-mechanical properties of spin and angular momentum. If there is sufficient exchange energy between neighboring dipoles, they will interact and spontaneously aligned parallel or anti-parallel, forming the magnetic domains, resulting in ferromagnetism or anti-ferromagnetism respectively. Paramagnetic behaviour can also be observed in

ferromagnetic materials only above their Curie temperature, and in anti-ferromagnetic above their Neel temperature.

In general, the paramagnetic effects are quite small and thus possess the magnetic susceptibility of the order of 10^{-3} to 10^{-5}, while it is high as 10^{-1} for synthetic paramagnets such as ferrofluids. For low levels of magnetization, the magnetization of paramagnets is approximated by Curie's law:

$$M = \frac{C.B}{T}$$

where, ***M*** *is the resulting magnetization*

B *is the magnetic flux density of the applied field in Tesla*

T *is absolute temperature, measured in Kelvin*

C *is a material-specific Curie constant*

1.2.3 FERROMAGNETISM

A property exhibited by certain metals, alloys and compounds of the transition metals such as iron, rare-earth and actinide elements that are below a certain temperature called the Curie temperature, the atomic magnetic moments tend to line up in a common direction [3]. Ferromagnetism is characterized by the strong attraction of one magnetized body for another. Atomic magnetic moments arise when the electrons of an atom possess a net angular momentum magnetic moment. The combined effect of the atomic magnetic moments can give rise to a relatively large magnetization for a given applied field. Above the Curie temperature, a ferromagnetic substance behaves as paramagnetic. Thus susceptibility approaches the Curie-Weiss law. The Curie temperature marks a transition between order and disorder of the alignment of the atomic magnetic moments. The ferromagnetic possess a spontaneous magnetization in the absence of an applied magnetic field below the Curie temperature. But under the

application of a weak magnetic field, the magnetization increases rapidly to a high saturation magnetization, which is in general a function of temperature.

1.2.4 ANTI-FERROMAGNETISM.

It is seen that ferromagnetism is due to the exchange interaction or exchange field which arises when the wave functions of the two atoms overlap [4]. Thus gives rise to an exchange energy. This exchange energy is positive when neighboring spins are parallel which leads to a ground state in which the neighboring spins are anti- parallel and hence there is a co-operative alternating alignment below a certain temperature T_N known as the Neel temperature. In these crystals, the alternate atoms have their spins parallel to each other but not the adjacent atoms. Such crystals can be considered to be composed up of two inter – penetrating sub-lattices A and B. One sub–lattice gets aligned in one direction, whereas the second in the other. Such substances are known as anti-ferromagnetic.

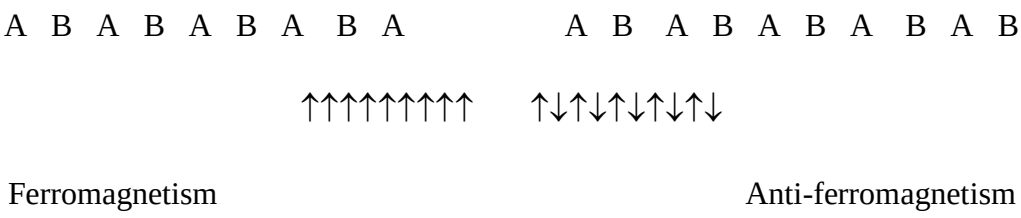

Fig 1.1 Parallel and anti-parallel spin alignment

In the absence of the external magnetic field, below the Neel temperature, the net magnetic moment is zero. The phenomenon of anti-ferromagnetism can be analyzed by assuming that alternate lattice points are occupied by atoms A and B with anti-parallel spins. Let the average magnetic moment field at the sites of atoms A and B respectively will be

$$\mathbf{B_A = B_0 - \lambda_A M_B}$$

and $$\mathbf{B_B = B_0 - \lambda_B M_A}$$

where B_0 is the external applied magnetic field, λ_A,λ_B constants independent of temperature and B_A and B_B the total magnetic field for the A and B sets of atoms respectively. For temperatures above T_N, the Neel temperature, according to Curie law, we have

$$\chi = \frac{c}{T+T_n}$$

where T_n is the Neel temperature. Thus in the case of anti-ferromagnets χ_m is inversely proportional to $\mathbf{T + T_C}$. When a magnetic field is applied, small magnetization in the direction of the field is developed. This magnetization increases as the temperature of the specimen is increased. With further increase of temperature, the interaction between sub-lattices becomes less effective and the susceptibility increases. For a particular temperature the susceptibility becomes maximum and above this temperature it starts decreasing. This critical temperature at which the susceptibility is maximum called Neel temperature. Above the Neel temperature spins are free and thus anti-ferromagnetic become paramagnetic. The peak occurring in the curve at $\mathbf{T = T_C}$ is most characteristic feature of anti-ferromagnetic. The susceptibility of anti-ferromagnetic at $\mathbf{T = T_N}$ is not infinite.

It means that at temperature below $\mathbf{T_C = T_N}$ the sets of atoms A and B are spontaneously magnetized in the opposite direction and the net magnetization is zero. This is why such materials are known as anti-ferromagnetic. In anti-ferromagnetic, the crystal field aligns the magnetic moments along a preferred direction below T_C. A field applied perpendicular to this direction is associated with a susceptibility $\chi_\perp$ which is independent of $\mathbf{T\ (T < T_C)}$ while a field applied parallel to this direction is associated with a susceptibility $\chi_{||}$ which is equal to $\chi_\perp$ at $\mathbf{T = T_C}$ but decreases to zero as $\mathbf{T \rightarrow 0\ K.}$

1.2.5 FERRIMAGNETISM

In physics, a ferrimagnetic material is one in which the magnetic moment of the atoms on different sub-lattices are opposed, as in anti-ferromagnetism; however, in ferrimagnetic materials, the opposing moments are unequal and a spontaneous magnetization remains [5]. This happens when the sub-lattices consist of different materials or ions (such as Fe^{2+} and Fe^{3+}).

Ferrimagnetic materials are like ferromagnetic, where they hold a spontaneous magnetization below the Curie temperature, and show no magnetic order (are paramagnetic) above this temperature. However, below the Curie temperature at which the two sub-lattices have equal moments, resulting in a net magnetic moment of zero; this is called the magnetization compensation point. This compensation point is observed easily in garnets and rare earth–transition metal alloys. Furthermore, ferrimagnetic may also exhibit an angular momentum compensation point at which the angular momentum of the magnetic sub-lattices is compensated. This compensation point is a crucial point for achieving high speed magnetization reversal in magnetic memory devices.

Ferrimagnetism is exhibited by ferrites and magnetic garnets. The oldest-known magnetic substance, magnetite (Fe_3O_4), is ferrimagnetic. It was originally classified as a ferromagnetic before Neel's discovery of ferrimagnetisms and anti-ferromagnetism. Some ferrimagnetic materials are YIG (yttrium iron garnet) and ferries composed of iron oxides and other elements such as aluminum, cobalt, nickel, manganese and zinc.

Ferrimagnetic materials have high resistivity and have anisotropic properties. The anisotropy is actually induced by external applied field. When the applied field aligns the magnetic dipoles it causes a net magnetic dipole moment and causes the magnetic dipoles it to presses at a frequency controlled by the applied field called Larmour or precession frequency. A microwave signal circularly polarized in the same direction as this precession strongly interacts with the dipole moments; when it is in opposite direction the interaction is very low. When the interaction is strong the microwave signal can pass through the material. This

directional property is used in the construction of microwave devices like isolators, circulators and gyrators.

1.3 SINGLE-DOMAIN PARTICLES

Domain is groups of spins all pointing in the same direction separated by domain walls and acting cooperatively. The motion of domain walls is a primary means of reversing magnetization. Experimental investigation of the dependence of coercivity on particle size showed a behavior similar to that schematically illustrated in Fig.1. 2 [6].

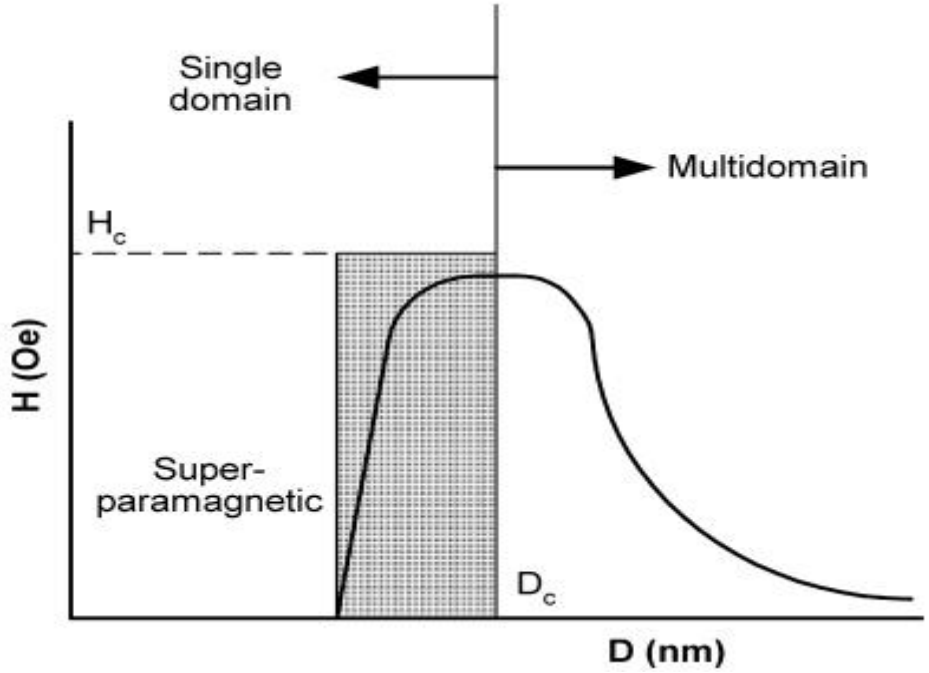

Fig. 1.1 Qualitative illustration of the behavior of the coercivity in ultrafine systems as the particle size changes, where *H* is the magnetic field amplitude (Oe) and *D* is the particle diameter (nm).

It was found that the coercivity *Hc* increases with decreasing grain size *D* down to values of about 40nm. The increase of *H*c is proportional to 1/*D*. This attributes

that in small particles the formation of a closed magnetic flux becomes energetically less favorable so that the magnetic domain size with a uniform magnetization becomes more and more identical. This grain size is defined by the first critical size *D*, which is characteristic of each material, where the multidomain materials change to a monodomain material. This leads to a strong increase of the coercivity because a change of magnetization in this case cannot happen only by shifting the domain walls which normally requires only a weak magnetic field. As the size of magnetic element scales below 20nm, the transformation from ferromagnetic to superparamagnetic behavior occurs. In the superparamagnetic state of the material, the room temperature thermal energy over comes the magnetostatic energy well of the domain or the particle, resulting in zero hysteresis. In other words,

Although the particle itself is a single-domain ferromagnet, the ability of an individual magnetic "dot" to store magnetization orientation information is lost when its dimension is below a threshold. Consequently, the magnetic moments within a particle rotate rapidly in unison, exhibiting the superparamagnetic relation phenomenon.

1.4 PROPERTIES OF MAGNETIC MATERIALS

1.4.1 SATURATION MAGNETIZATION

The saturation magnetization M_S is a measure of the maximum amount of field that can be generated by a material. It will depend on the strength of the dipole moments on the atoms that make up the material and how densely they are packed together. The atomic dipole moment will be affected by the nature of the atom and the overall electronic structure. The packing density of the atomic moments will be determined by the crystal structure (i.e. the spacing of the moments) and the presence of any non-magnetic elements within the structure. At finite

temperatures, for ferromagnetic materials, M_S will depend on how well these moments are aligned, as thermal vibration of the atoms causes misalignment of the moments and a reduction in M_S. For ferrimagnetic materials, all moments are aligned parallel even at zero Kelvin and hence M_S will depend on the relative alignment of the moments as well as the temperature.

1.4.2 CURIE TEMPERATURE

The Curie point of a ferromagnetic material is the temperature above which it loses its characteristic ferromagnetic ability. At temperatures below the Curie point, the magnetic moments are partially aligned within magnetic domains in ferromagnetic materials. As the temperature is increased from below the Curie point, thermal fluctuations increasingly destroy this alignment, until the net magnetization becomes zero at and above the Curie point material is purely paramagnetic. At temperatures below the Curie point, an applied magnetic field has a paramagnetic effect on the magnetization, but the combination of paramagnetic with ferromagnetic leads to the magnetization following a hysteresis curve with the applied field strength. The Neel temperature, T_N is the temperature at which an anti-ferromagnetic material becomes paramagnetic that is, the thermal energy becomes large enough to destroy the macroscopic magnetic ordering within the material.

1.4.3 MAGNETIC ANISOTROPY

In a crystalline magnetic material, the magnetic properties will vary depending on the crystallographic direction in which the magnetic dipoles are aligned. A measure of the magneto crystalline anisotropy in the easy direction of magnetization is the anisotropy field, *Ha*, which is the field required to rotate all the moments by 90^o as one unit in a saturated single crystal. The anisotropy is caused by a coupling of the electron orbitals to the lattice, and in the easy direction of magnetization this coupling is such that these orbitals are in the lowest energy state. The easy direction of magnetization for a permanent magnet,

based on ferrite or the rare earth alloys, must be uniaxial, however, it is also possible to have materials with multiple easy axes or where the easy direction can lie anywhere on a certain plane or on the surface of a cone. The fact that a permanent magnet has uniaxial anisotropy means that it is difficult to demagnetize, as it is resistant to rotation of the direction of magnetization.

1.4.4 HYSTERESIS LOOP

Hysteresis is well known in ferromagnetic materials. When an external magnetic field is applied to a ferromagnetic, the atomic dipoles align themselves with the external field. Even when the external field is removed, part of the alignment will be retained and thus the material has become magnetized. The relationship between magnetic field strength *H* and magnetic flux density *B* is not linear in such materials. If the relationship between the two is plotted for increasing levels of field strength, it will follow a curve up to a point where further increases in magnetic field strength will result in no further change in flux density. This condition is called magnetic saturation. If the magnetic field is now reduced linearly, the plotted relationship will follow a different curve back towards zero field strength at which point it will be offset from the original curve by an amount called the remanent flux density or remanence. If this relationship is plotted for all strengths of applied magnetic field the result is a sort of S- shaped loop. The thickness of the middle bit of the S describes the amount of hysteresis, related to the coercivity of the material. Its practical effects might be cause of a relay to be slow to release due to the remaining magnetic field continuing to attract the armature when the applied electric current to the operating coil is removed.

1.4.5 REMANENCE

Remanence is the magnetization left behind in a medium after an external magnetic field is removed. It is denoted in equations as M_r. The remanence magnitude can be taken from a hysteresis loop at the intersections of the loop with the vertical magnetization axis.

1.4.6 COERCIVITY

In materials science, the coercivity ferromagnetic materials also called the coercive field, is the intensity of the applied magnetic field required to reduce the magnetization to zero after the magnetization of the sample has been driven to saturation. Coercivity is usually measured in oersted or ampere/meter units and is denoted H_C. When the coercive field of a ferromagnetic is large, the material is said to be a hard or permanent magnet.

1.4.7 MAGNETOSTRICTION

If the substance, exposed to a magnetic field it cause of dimensional changes. This effect is called magnetostriction [7]. The fractional change in length ΔL/L is simply a strain and to distinguish it from the strain ε caused by an applied stress, we give the magnetically induced strain a special symbol λ

$$\boldsymbol{\lambda = \Delta L/L}$$

The value of λ measured at magnetic saturation is called saturation magnetostriction $\lambda_{s.}$ and its value depends on extent of magnetization and on applied field.

1.5 FERRITES

Ferrites are chemical compounds with the formula AB_2O_4, where A and B represent various metal cations; usually including iron [8]. Ferrites are a class of spinels i.e. materials that adopt a crystal motif consisting of cubic closed pack oxides with A cations occupying $1/8^{th}$ of the octahedral voids and B cations occupying half of the octahedral voids. For inverse spinel structure, half the B cations occupy tetrahedral sites and both the A and B cations occupy the octahedral sites. Divalent, trivalent and quadrivalent cations can occupy the A and B sites and they include Mg, Zn, Fe, Mn, Al, Cr, Ti and Si.

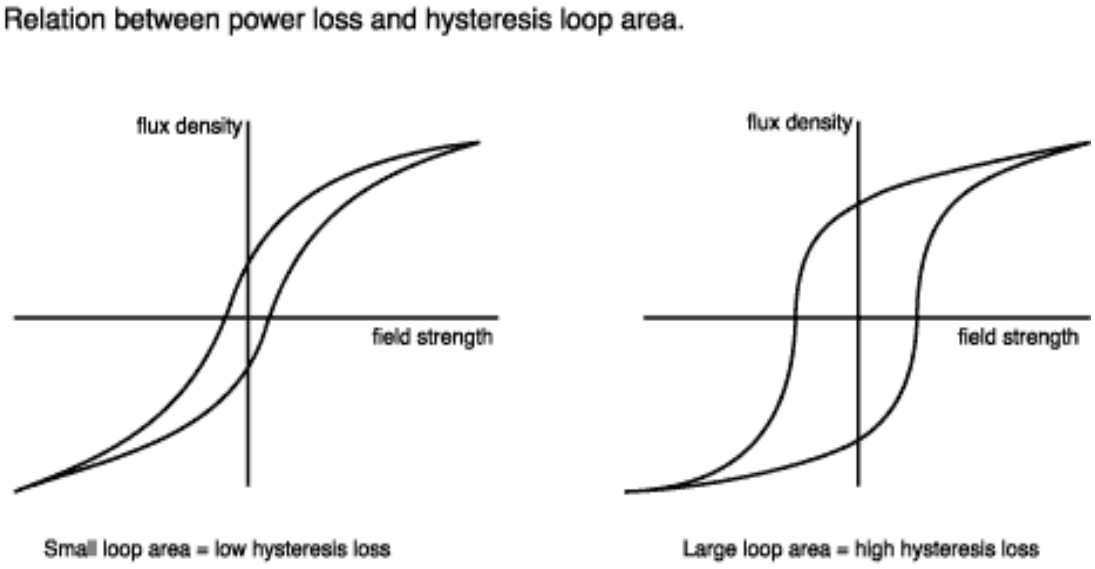

Figure 1.2 Hysteresis Loop for Soft and Hard Ferrite

Ferrites are usually non-conductive ferromagnetic ceramic compounds derived from iron oxides as well as oxides of other metals. Like most other ceramics, ferrites are hard and brittle. Based on the magnetic properties, ferrites are often classified as soft and hard ferrites as shown in Figure 1.2.

1.5.1 SOFT FERRITES

These are characterized by a small value of coercivity so they cause low hysteresis loss at high frequency owing to which they are widely used in electromagnetic cores of transformers, switching circuits in computers and RF inductors, e.g., Lithium ferrite, Nickel ferrite and Mn-Zn ferrite.

1.5.2 HARD FERRITES

These are characterized by a large value of retentivity and coercivity after magnetization so they find applications as permanent magnets in radios, e.g., Barium and Strontium ferrite. Maximum magnetic field is about 0.35 T and magnetic field strength is about 30 to 160 KA - turns/m. Ferrites are ferrimagnetic materials that are typically oxides of mixed transition metals involving the iron. For example, MnFe2o4 and Mg-Zn ferrite is $Mn_{1-x}Zn_xFe_2O_4$ they are usually insulater in nature, like most other ceramics, hard and brittle. In terms of the magnetic properties, ferrites are often classified as "soft" and "hard" which refers to their low or high coercivity of their magnetism respectively. Ferrites are like most other ceramics, hard and brittle. In terms of the magnetic properties, ferrites are often classified as “soft” and “hard” which refers to their low or high coercivity respectively. These ceramic materials are used in application ranging from magnetic components in microelectronics. Most of the ferrite particles used in synthesize magnetic fluid posses a spinel structure. This structure consist of a cubic closed packed case of oxygen ions with the metallic ions occupying the tetrahedral A and octahedral B interstitial site.

1.6 STRUCTURE OF UNIT CELL OF SPINEL FERRITE

The unit cell of a spinel ferrites consists of 32 oxygen, 16 trivalent iron, and 8 divalent metal irons. The most important feature of the unit cell is that its array of oxygen ions leaves open two kinds of interstices, which can be filled by the metal ions. These interstices are referred to as tetrahedral or A sites and octahedral or B sites. Fig. 1.4 shows the unit cell of spinel structure. There are two groups of four cubes (octants). The ionic positions are different in two octants sharing a face or a

corner and the same in two octants sharing an edge. Thus, to give a complete picture, it is necessary only to show the positions of the ions in two adjacent octants. Note that each octants contains, in the center a metal ion (small green sphere) surrounded by the tetrahedral of oxygen ions, this ion is said to occupy an A site. The right hand octant shows four metal ions (small red spheres) each surrounded by an octahedran (one of which is shown) formed by six oxygen ions. Such ions are said to occupy B sites. In a unit cell, there are 64 A sites, 8 of which are occupied, and 32 B sites, 16 of which are occupied. The divalent metal ions commonly used in ferrites can be classified roughly into those preferring B sites Co, Fe, Ni and those preferring A sites Mn and Zn. In the normal spinel structure the 8 divalent metal ions go into the A sites and the 16 trivalent iron ions have preference for B sites, they will displace eight of the trivalent iron ions which with go over into the A sites. This results in an inverted spinal. As two ionic species are then distributed over the octahedral sites a certain number of randomness may be present, contributing to the line width (loss) of the materials. These are however, limiting cases [25].

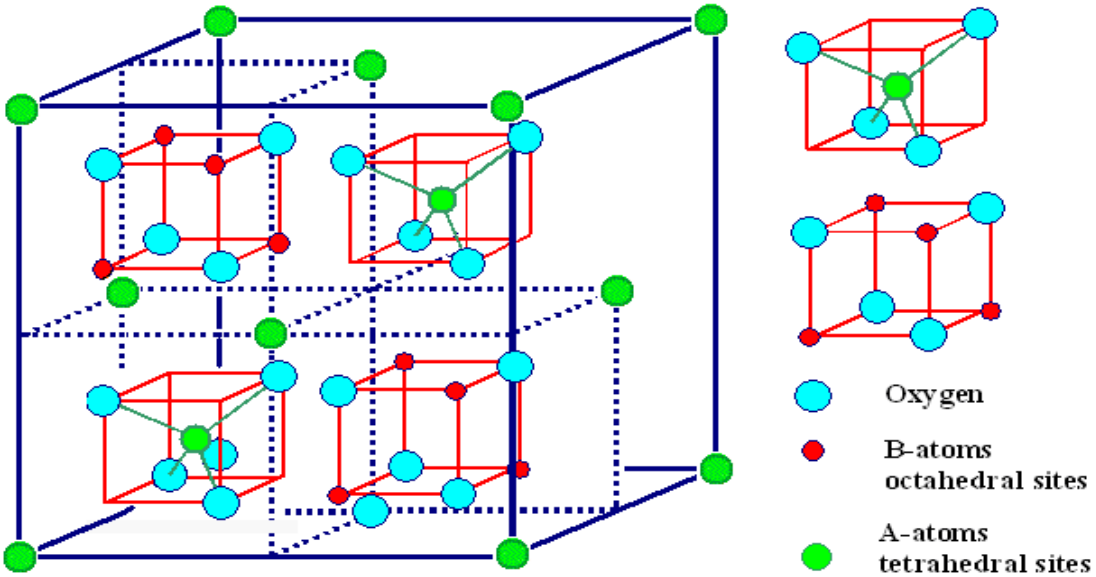

AB_2O_4 spinel The red cubes are also contained in the back half of the unit cell

Fig 1.3 :- Structure of unit cell of spinel ferrite

1.7 SUBSTITUTION IN SPINELS

The situation is further complicated in the case of substituted ferrites. In these materials, some of the ferric iron ions are replaced by trivalent ions of another metal. The effect on the magnetization depends on the site preferred by the substituent, e.g. Al prefers octahedral coordination and therefore reduces the magnetization of the substituent ferrite, at least for small Ga concentration. It is not easy to predict the ion distribution in advance [9].

1.8 SPINEL STRUCTURES

In the spinel structure the oxygen ions form an fcc lattice and the A^{+2} valence and B^{+3} valence ions occupy tetrahedral and octahedral interstitial sites, depending on the particular type of spinel.

1.8.1 NORMAL SPINEL STRUCTURE

In the spinel structures unit cell there are 8 $MO.Fe_2O_3$ molecules. In this structure the eight M^{+2} ions occupy eight tetrahedral sites and the 16 Fe^{+3} ions occupy 16 octahedral sites [10]. In other words, in this structure, the non-magnetic ions occupy the A sites and consequently there is no AB interaction. The negative BB interaction now makes itself felt and the trivalent irons ions align themselves in an anti-parallel fashion, producing zero net magnetization [9].

1.8.2 INVERSE SPINEL STRUCTURE

In the inverse spinel structure there are $8M^{+2}$ ions which occupy 8 octahedral sites and the 16 Fe^{+3} ions are divided, the 8 occupy octahedral sites and 8 tetrahedral sites as shown in table 1 [10].

Table 1:- Metal ion arrangements in spinel ferrite unit cell with composition $MO.Fe_2O_3$

Types of interstitial site	Number available	Number occupied	Normal spinel	Inverse spinel
Octahedral	64	8	$8M^{+2}$	$8Fe^{+3}$
Tetrahedral	32	16	16 Fe_{+3}	$8Fe^{+3}$ $8M^{+2}$

we may say that, in the inverse or inverted structures, the nonmagnetic ions occupy eight B sites, whereas the iron is evenly divided between the two lattice sites The AB interaction, overriding the AA and BB interactions, leads to a parallel arrangement within each sub lattice. As the divalent ions have no magnetic moment, the net magnetization vanished [9].

1.8.3 PARTIALLY INVERTED STRUCTURES

In this type of structure, such as Mg-ferrite the trivalent iron is un-symmetrically distributed between the two types of sites and if the AB interaction is dominant,there will be a net magnetization [10].

1.9 NANO-MAGNETIC MATERIAL

Nanotechnology is the understanding and control of matter at dimensions of roughly 1–100 nm, where unique phenomena enable novel applications. The physical and chemical properties of the nanomaterials tend to be exceptionally closely dependent on their size and shape or morphology. As a result, materials scientists are focusing their efforts on developing simple and effective methods for fabricating nanomaterials with controlled size and morphology and hence tailoring their properties. An important aspect of the nanoscale is that smaller the

size of the particle, larger its surface area. At the nanoscale, properties like electrical conductivity and mechanical strength are not the same as they are at bulk size, but changes dramatically. Recently, the synthesis of nano-magnetic materials has been a field of intense study, due to the novel mesoscopic properties shown by particles of quantum dimensions located in the transition region between atoms and bulk solids [11]. Quantum size effects and the large surface area of magnetic particles dramatically change some of the magnetic properties and exhibit superparamagnetic phenomena and quantum tunneling of magnetization, because each particle can be considered as single magnetic domain Magnetic nanoparticles have attracted increasing interest both in fundamental science and in technological applications because of their various useful properties in the recent trend of nanotechnology.

A variation in particle size can also modulate the physical properties even without varying the composition. As the size of the particles decreases below 100 nm, a large fraction of the constituting atoms are found on the surface of the nanocrystals; this induces significant changes in the magnetic structure and properties of the materials at nanoscale as compared with their bulk counterpart. Specially, the domain wall structure encountered in the bulk crystalline ferrites is replaced by a single domain structure characteristic of each particle, thus leading to new phenomena such as superparamagnetism, extra anisotropy contributions and spin canting [12].

Magnetic nanoparticles of spinel ferrites are of great interest in fundamental science, especially for addressing the fundamental relationships between magnetic properties, their crystal chemistry and structure. Crystal chemistry shows how the chemical composition (chemical formula), internal structure and physical properties of minerals are related each other. Spinel ferrites have been investigated in recent years for their useful electrical and magnetic properties and applications in information storage systems, magnetic bulk cores, magnetic fluids, microwave absorbers and medical diagnostics. The synthesis and magnetic structure characterization of ferrites have been investigated with much interest [12–14] and a lot of attention has been focused on the preparation and characterization of

superparamagnetic metal oxide nanoparticles of spinel ferrites with chemical formula, $MeFe_2O_4$ (where Me = Co, Mg, Mn, Zn, etc.) [15–20].

Nanophase materials with an average grain size in the range of 1 to 50 nm have attracted research interest for more than a decade since their physical properties are quite different from that of their bulk micron-sized counterparts because of the large volume fraction of atoms that occupies the grain boundary area [21-22]. This is a new class of materials which being used in important applications like high frequency transformers, ferrofluids, pigments in paints and ceramics, biomedical applications like drug delivery system, hyperthermia, NMR, high density magnetic recording and dye-sensitized solar cells [23-24].

The surface area of the nanostructures materials is large as the grain sizes are small. The increase in the interfacial energy due to defects, dislocations and lattice imperfections leads to changes in various physical properties and hence one can tailor make the materials with specific properties. Almost 50 % of the atoms reside in the grain boundary area when the grain size is reduced to less than 10 nm whereas it is only 1-3 % when the grain size is 100 nm [25, 26]. Since a large fraction of atoms is present at the grain boundaries, the nanocrystalline materials exhibit enhanced diffusivity.

The magnetic materials are classified into two groups such as soft and hard magnetic materials. Soft magnetic materials have low magneto crystalline anisotropy resulting in reduced coercivity and high permeability such as melt-spun (Fe-Si-B-Nb-Cu) and (Fe-M-B-sCu) alloys. The high Curie temperature (Fe-Co-Cu-Zr) alloys are used in the high application. The saturation magnetization for the nanocrystalline ferrites, in general, is found to be lower compared to their bulk value, which is attributed to surface spin effects. In some cases an enhancement in the saturation magnetization is observed due to the change in cation distribution which depends on the crystal field stabilization energy of the cations. Apart from grain size, the cation distribution, which depends on the synthesis condition, is found to play a major role in the observed changes in their magnetic properties. The high coercivity of the hard magnetic materials arises from the large magneto crystalline anisotropy of the materials with a non-cubic structure.

The nano magnetic materials can be synthesized with varying grain size using the techniques like mechanical milling, sol gel method, laser ablation method, oxidation method, reverse micelle polyol process and co precipitation method etc. The co precipitation technique has been used in the synthesis of $CdFe_2O_4$, $ZnFe_2O_4$, Ni-$ZnFe_2O_4$ and $MgFe_2O_4$ by various researchers. The remarkable properties of the nanomagnetic materials are interested in understanding the effect of particle grain size on the magnetic properties of both soft and hard magnetic materials. In the present study, Mn-Zn nano-ferrite particles have been synthesized by chemical co-precipitation method.

Further the characterization of these materials the for structural, physical and magnetic properties of is done in order to understand the correlation between the properties and the particle size. For this various analytical techniques such as X-ray diffraction (XRD), electron paramagnetic resonance (EPR) spectroscopy and transmission electron microscopy (TEM) have been used. Characteristics of the nanostructures materials like line broadening in the X-ray peak are used to estimate the average grain size using the X-ray diffraction. The surface morphology and shape of the nanoparticles are examined using transmission electron microscopy. The relaxation effects, magnetic properties of and spin concentration occurring in the nanoparticles on size reduction are investigated using electron paramagnetic resonance spectroscopy.

1.10 Ferro Magnetic Fluid

Ferrofluids are the colloidal suspension of ferro/ferri-magnetic particles of size range 2-10nm, coated with surfactant chains in a carrier liquid. It is stable against gravitational as well as magnetic field gradient

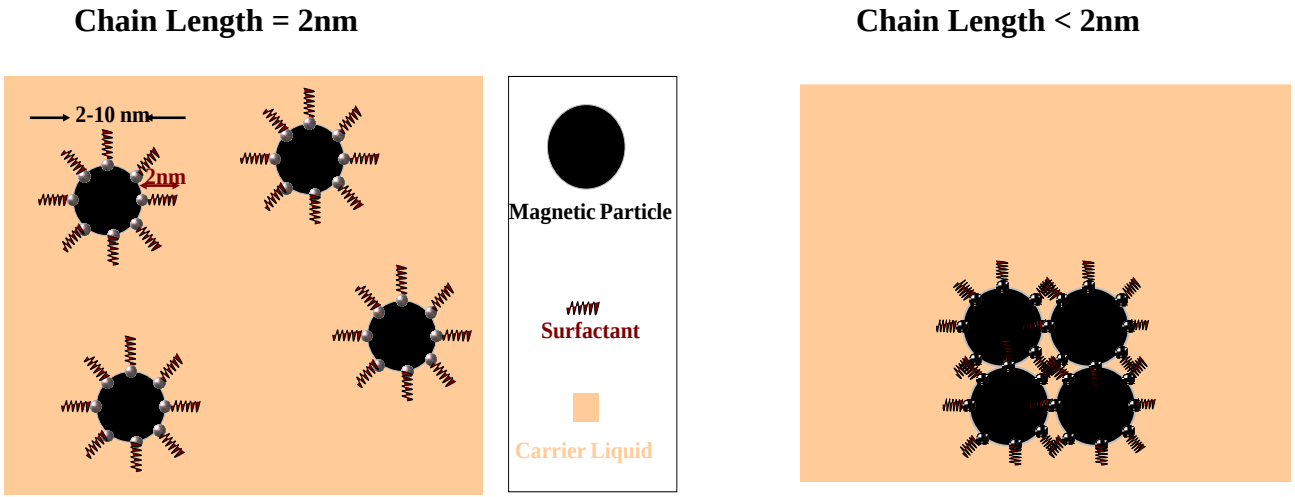

Fig 1.4 Ferrofluid = 5-10% Superparamagnetic Particles + 10% Surfactant + 80-85% Carrier Liquid

In the case of Ferro fluid the surfactant may be kerosene, hexadecane and oleic acid Surfactant having long chain hydrocarbon consist of polar head called hydrophobic part and

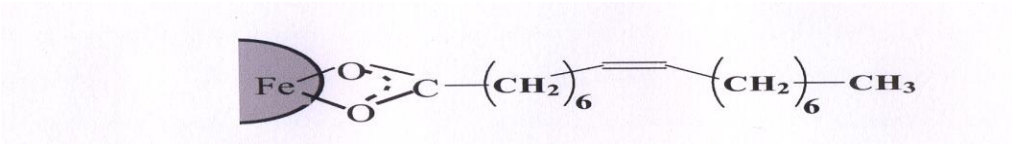

Fig 1.5 structure of oleic acid

a more extended hydrocarbon tail called hydrophilic part[27] .Oleic acid is one of the most widely used surfactants.

PROPERTIES OF FERROFLUID

- Stick to Magnets.
- Take on 3-Dimensional Shape on applying a Magnetic Field.
- Change Density in Proportion to applied Magnetic Field Strength.

1.10.1 MAGNETIC BEHAVIOR OF FERROFLUID

In the absence of magnetic field, the magnetic moments of the particles are randomly distributed and the field has no net magnetization. When a magnetic field is applied to a ferrolluid, the magnetic moments of the particles orient along the fields lines almost instantly Tthe magnetization of ferrofluid responds immediately to the changes in the applied magnetic field and when the applied field is removed, the moments randomized quickly.

In a gradient field the whole fluid responds as a homogeneous magnetic liquid, which moves to the region of highest flux. This means that ferrofluids can be precisely positioned and controlled by an external magnetic field and the magnetization value of the fluid. This means that the retention force of a ferrofluid can be adjusted by changing either the magnetization of the fluid or the magnetic field in the region.

1.11 APPLICATION OF FERROFLUID

There are a whole host of other applications for ferrofluid. Many are still at the R&D stage but some have already achieved a degree of commercial success. Ferrotec carries out research into new applications for ferrofluids both on its own

and through strategic partnerships with other companies. Other application areas in which ferrofluids have been used include material recycling, power and distribution transformers quiet solenoids sensors and switches.

1.11.1 MATERIAL RECYCLING

Ferrofluid has a unique property in that applying magnetic field to the ferrofluid can increase its apparent density. This physical characteristic creates the ability to separate objects of different density through floatation or sinking. Ferrofluids have been used for years in material separation processes in the mining industries, although with limiting economic advantage. Ferrofluidics has been working with material recycling and mining industry leaders to commercialize this application. To enhance the economic viability of these processes, ferrofluidics has developed patent- pending process for the reclamation and reconstitution of ferrofluids. This innovation creates economic advantage for the separation industries to enhance the existing separation performance characteristics of the material.

1.11.2 ELECTRICAL TRANSFORMERS

Ferrofluidics Corporation has been working in partnership with a major manufacturer of electrical power equipment, to develop ferrofluid for liquid-filled transformer applications.Ferrofluids have been shown to provide both thermal and dielectrical benefits to transformers. Ferrofluid can be utilized to improve cooling by enhancing fluid circulation within transformer winding. Ferrofluid can also be applied to increase transformer capacity to withstand lighting impulses, while also minimizing the effect to moisture on typical insulating fluids. The benefits of ferrofluid may be utilized to design smaller, more efficient new transformers, or to extend the life or loading capability of existing units.

1.11.3 THERMAL CONDUCTIVITY OF FERROFLUIDS

The thermal conductivity of kerosene based ferrofluids can be enhanced by using small but permanent magnetic field different orientations. In the absence of a

magnetic field, the magnetic moments of the particles are randomly distributed and the fluid has no net magnetization. The magnetization of the ferrofluid respond immediately to the changes in the applied magnetic field and when the applied field is removed, the moment randomize quickly. Tomorrow's coolants for the electronic devices and would come from magnetic nanofluid and nanofluid are more conducting than air. With the size of electronic chips ever shrinking, there is great compulsion to find very efficient heat sinks. Such heat can be made using high heat dissipation finds application in new generation devices such as Nanoelectrochemical systems (NEMs) and Micro electrochemical systems (MEMs). One way of extracting heat from equipment which heated up by functioning and so keeping it not too hot, is by using a good heat conductor which connects the equipment to some mass which has much bigger heat capacity and perhaps, much bigger open surface to dissipate heat. In some cases the good heat conductor must not be a solid, because it would block the equipment's operation. One way to achieve the desired goal is by using a ferrofluid as heat conductor. A non magnetic liquid would flow away from the place where it is supposed to operate. A good example is a loudspeaker, whose coil heats up by functioning and the ferrofluid is kept in place by the magnetic field of the magnet which is fixed on the loudspeaker's horn. Now a day's most of the high power loudspeakers are equipped with ferrofluid. The presence of the fluid around the coil improved also the quality of the speaker because it damps unwanted resonances, which would produce a very unpleasant noise.

1.11.4 INERTIAL AND VISCOUS DAMPER

We mentioned above that magnetic fluids are used also as damper in loudspeakers. A more direct use for damping unwanted vibrations is associated to their use as inertial and viscous damper for motors, mainly stepper motors. For this purpose use is made of the unique property of magnetic fluid that can keep magnet, whose mass density is bigger than that of the fluid, floating in it, with part of its volume above the liquid's surface. This is because the magnetic field gradient pulls the magnetic fluid to the region under the immersed pole of the magnet, causing a pressure (magnetic pressure) which pushes the magnet up. The

equilibrium is established when the magnet's weight is counterbalanced by this magnetic pressure and the hydrostatic pressure. A stepper motor operated at its natural frequency may experience excessive setting time, vibration and acoustic noise. A damper absorbs the unwanted vibration by shearing effect which produces a torque that opposes the oscillatory motion. The damper has non-magnetic housing which attaches to the motor shaft. Inside the housing is an inertial mass which levitates on ferrofluid, thus eliminating the need for bearings to supports the mass [28].

1.11.5 QUIET SOLENOIDS

The introduction of a ferrofluid into a solenoid dramatically reduces the noise level of certain equipment, such as home care kidney machines. This in turn reduces the need for noise suppression insulation, allowing a more cost effective and simpler design that is more portable. In addition to the obvious benefits of quieter operation and portability, the ferrofluid based solenoids makes the equipment more reliable.

1.11.6 SENSORS & SWITCHES

The unique properties of magnetic fluid make it a feasible technology for some sensor and switch application. The use of ferrofluid may enhance the motion sensitivity in some sensing applications. Products being evaluated for ferrofluid application include inclinometers, accelerometers and flow meters, tilt, vibration, pressure and level sensors, and various switches.

1.11.7 AUDIO FERROFLUID

As the global leader in ferrofluid products, Ferrotec has been supplying ferrofluid to audio speaker manufacturers since the 1970s. Ferrofluid enables audio speaker to function more efficiently, with improved audio response and better power handling. For audio speaker manufacturers, Ferrotec ferrofluid also provides significantly better manufacturability for improved quality and higher manufacturing yields. Audio ferrofluids are based on two classes of carrier liquid: synthetic hydrocarbons and esters. Both oils possess very low volatility and high

thermal stability. The choice of fluid dictated by the environmental consideration of the application (e.g. humidity, adhesives and contact with the water, solvent vapors and reactive gasses) combined with the best balance of magnetization and viscosity values to optimize the acoustical performance. By varying the quantity of magnetic material in a ferrofluid and by using different carrier liquids, it can be tailored to meet a variety of needs. The saturation magnetization is determined by the nature of the suspended magnetic material and by the volumetric loading of the material. The physical and chemical properties such as density and viscosity correspond closely to those of the carrier liquid.

1.11.8 BIOMEDICAL APPLICATION

1.11.8.1 HYPERTHERMIA

Recently ferrorluid have also been used in biomedical field. Biological application using maghemite ferrofluids: magnetic cell sorting and magnetocytolysis were reported by Roger et al. Especially, treatment of cancer by magnetic hyperthermia, magnetic drug targeting eye surgeriesare gaining much attention in recent days. The property of ferrofluid absorbing electromagnetic energy at a frequency that is different from the frequency at which water absorbs energy allows one to heat up a localized portion of a living body, where ferrofluid has been injected.For example a tumor, without heating at the same time the surrounding parts of the body. A number of experiments, healing cancer tumors in rats and rabbits by this technique have been reported during the last few days [29]. In the year of 2004 a new important step was given in this direction where humans had their cancer tumour successfully treated by magnetic fluid hyperthermia (MFH). An experimental treatment of 15 patients in association with low dose radiotherapy, showed very good results; the treatment was well tolerated by the patients, leaving clear that it constitutes an important new weapon against cancer.

1.11.8.2 CONTRAST ENHANCEMENT FOR MAGNETIC RESONANCE IMAGING

It has been one of the most powerful diagnosis techniques used in medicine in recent years. Frequently, however, the differences are not strong enough to render well resolved images. If magnetic particles from a biocompatible ferrofluid are selectively absorbed by some kind of tissue, this will become very clearly visible by MRI. Moreover, different tissue uptake different amount of the magnetic particles, having the different values of T_2 and distinguishable images. Dextran coated iron oxide are compatiable and are excreted via the liver after the treatment they are selectively taken up by the reticuloendothelial system. This is important because tumor cells do not have the effective reticuloendothelial system of healthy cells so their relaxation is not altered by the contrast agent, which makes them distinguishable from the surrounding healthy cells. Pankhurst et al in a recent topical review on application of magnetic nanoparticles in biomedicine.

1.11.8.3 MAGNETIC SEPARATION OF CELLS

It is advantageous to separate out specific biological entities from their native environment, for different possible reasons in order to produce concentrated samples of these entities or to free an infected sample from them. Magnetic separation using bicompatible magnetic particle from ferrofluids is one way to achieve this. It is a two step process 1) fixing a magnetic particle to the desired biological entity, and 2) pulling the magnetic particles, together with their "prey" out of the native environment by the action of a magnetic field gradient. Fixing the magnetic particle to the biological entity id made possible by coating a particle by appropriate material, such as dextran, polyvinel alcohol and others [52]. Uses of cell separation include clean up bone marrow from cancer infected samples taken from a person, aiming to use the purified sample to the implanted again in the same person, avoiding in this way the rejection, very common when the implanted material comes from a different donor. In this case, magnetic

nanospheres are coated with monoclonal antibodies having an affinity for the tumor cells. When marrow removed from the patient is put in contract with the coated spheres in a liquid solution, the rumor cells selectively attach to the surface of the spheres, which are then magnetically separated from the solution [53].

Chapter 2

2. EXPERIMENTAL DETAILS

2.1 SYNTHESIS OF $Mn_xZn_{1-x}Fe_2O_4$ MAGNETIC NANO-PARTICLES

The magnetic nano-particles of $Mn_xZn_{1-x}Fe_2O_4$ particles with compositions (x = 0.1, 0.3, 0.5) have been synthesized by a chemical co-precipitation method [32,33]. Fig. 2.1 displays a flow chart showing various steps involved in the synthesis process. The starting materials used were AR grade $MnCl_2.2H_2O$, $ZnCl_2$, $FeCl_3$. These salts were dissolved in distilled water with constant stirring to get 5M solutions. For synthesis, equimolar solutions of $MnCl_2.2H_2O$, $ZnCl_2$, and $FeCl_3$ were mixed in their stoichiometric ratio and homogenized at 60°C. To this 25% ammonia solution was added drop by drop with constant stirring. The pH of the solution was maintained at 9.5. The mixture was then heated at 80°C for about one hour. This duration is sufficient for transformation of hydroxides into spinel ferrites (digestion step).

To prevent agglomeration a surfactant coating of oleic acid was made to the individual particles in the beginning itself. The precipitated particles were then washed several times with double distilled water to remove the salt residues and other impurities. It was further dried at 80°C to obtain the powder. During synthesis, the molar concentration, temperature, pH of the reaction mixture, etc. were optimized to get single-phase nano crystalline material. The samples were annealed at different temperature (573K, 773K, 973K, 1173K, and 1373K) in an air atmosphere for two hours using a Carbolite make high-temperature Muffle furnace. The samples were then characterized through various characterization techniques.

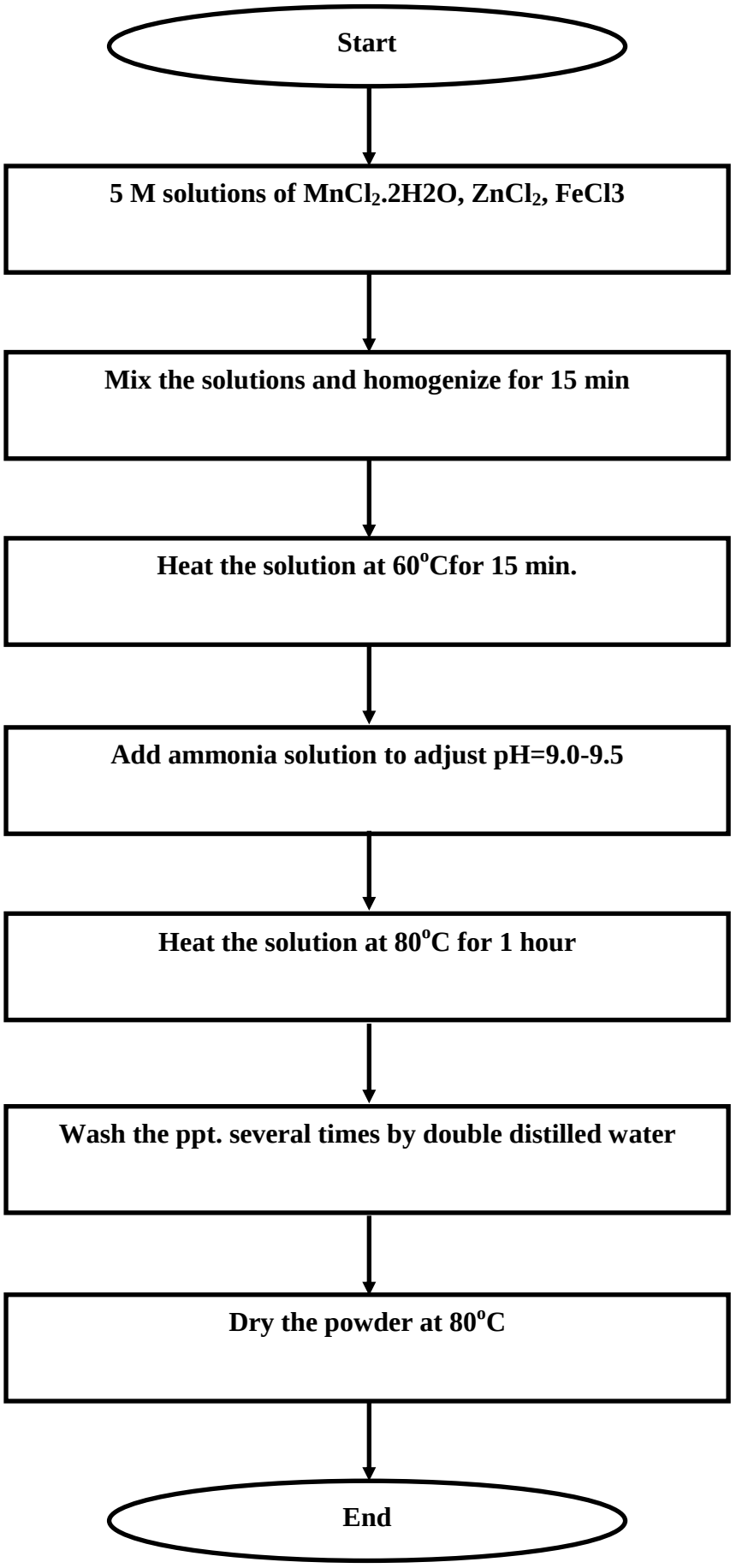

Fig 2.1: Flow chart of the synthesis of $Mn_xZn_{1-x}Fe_2O_4$ nanoparticles

2.2 FUNDAMENTAL MATERIALCHARACTERIZATION

2.2.1 X-Ray Diffraction (XRD)

The crystalline structures of various magnetic materials were investigated by Wide Angle X-Ray Diffraction (WAXD), using a powder X-Ray diffractometer (Rigaku make X-ray model) with Cu-$K_{\alpha 1}$ source at 40kv, 30mA as shown in Fig.2.2. All the samples were recorded in the 2θ regions of 20-70 (2θ) at a scan rate of 0.02° per second. The crystal structure, lattice parameters, strains and crystallite size were determined from these studies.

2.2: Rigaku-make powder x-ray diffractometer, National Physical Laboratory, New Delhi

X-ray Diffraction is a powerful technique used to uniquely identify the crystalline phases present in materials and to measure the structural properties such as the strain state, grain size, epitaxial, phase composition, preferred orientation, and

defect structure of these phases. XRD is also used to determine the thickness of thin films, multilayer and atomic arrangements in amorphous materials including polymers at interfaces. Figure 2.3 shows the basic features of an XRD experiment set up; the diffraction angle 2θ is the angle between the incident and diffracted X-rays [34-35]. Form 2θ values for reflection 'd' value were calculated using Bragg's equation and average crystallite size calculated of ferrite nanoparticles by Scherrer's equation.

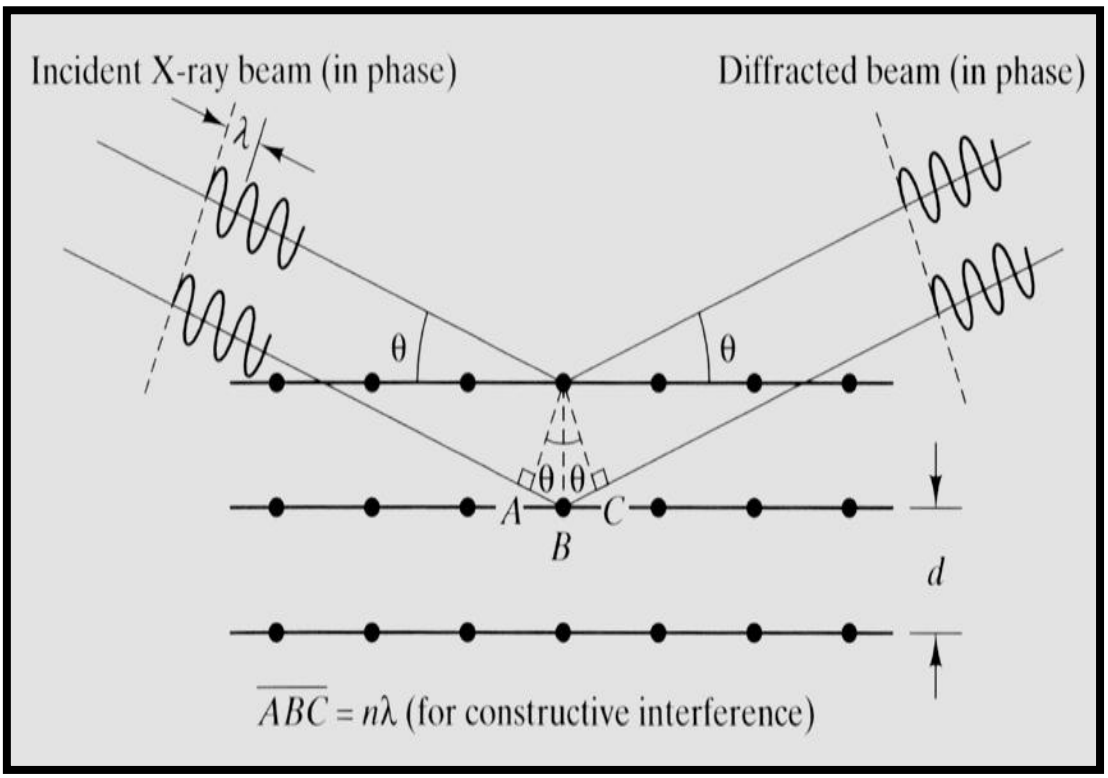

Figure 2.3: Basic features of a typical XRD experiment

Crystals consist of planes of atoms that are spaced a distance d apart Fig. 2.3, but can be resolved into many atomic planes, each with a different d-spacing. For the familiar cubic crystal, these form an orthogonal system. Any atomic plane can now be uniquely distinguished by its Miller indices. These are the three reciprocal intercepts of the plane with the a-, b-, and c-axes and are reduced to the smallest integers having the same ratio. The d-spacing between (hkl) planes is denoted by d_{hkl}.

$$d_{hkl} = a_o / \sqrt{h^2 + k^2 + l^2} \qquad \text{Equation (a)}$$

When there is constructive interference from X-rays scattered by the atomic planes in a crystal, a diffraction peak is observed. The condition for constructive interference from planes with spacing d_{hkl} is given by Bragg's law [36]:

$$n\lambda = (2)(d_{hkl})(\sin\theta_{hkl}) \qquad \text{Equation (b)}$$

where θ_{hkl} is the angle between the atomic planes and the incident and diffracted X-ray beam Fig.2.3. For diffraction to be observed, the detector must be positioned so that the diffraction angle is $2\theta_{hkl}$ and the crystal must be oriented so that the normal to the diffracting plane is coplanar with the incident and diffracted. Figure 2.4 shows several atomic planes and their d-spacing in a simple cubic (sc) crystal.

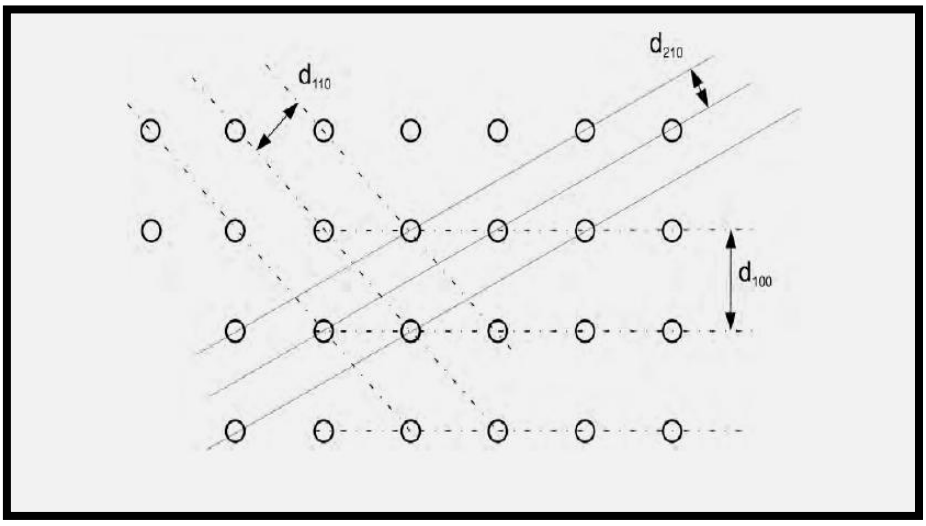

Figure 2.4: Atomic planes and their d-spacing in a simple cubic (SC) unit cell

2.2.2 EPR SPECTROSCOPY

The EPR measurements were carried out by Varian make E Line Century X-band EPR spectrometer (Model-E-112). The measurements were done at 9.36 GHz with modulation frequency 100 KHz. DPPH was used as standard reference material for field marker. The samples were taken in spin free quartz capillary tubes. These EPR spectra were analyzed to get the information about spin concentration and spin-spin relaxation.

Figure 2.5. Bruker make Q- X-band EPR Spectrometer, National Physical Laboratory, New Delhi

2.2.3 Origin of an EPR signal

Every electron has a magnetic moment and spin quantum number s = 1/2, with magnetic components m_s = +1/2 and m_s = -1/2. In the presence of an external magnetic field with strength B_0, the electron's magnetic moment aligns itself either parallel (m_s = -1/2) or antiparallel (m_s = +1/2) to the field, each alignment having a specific energy.

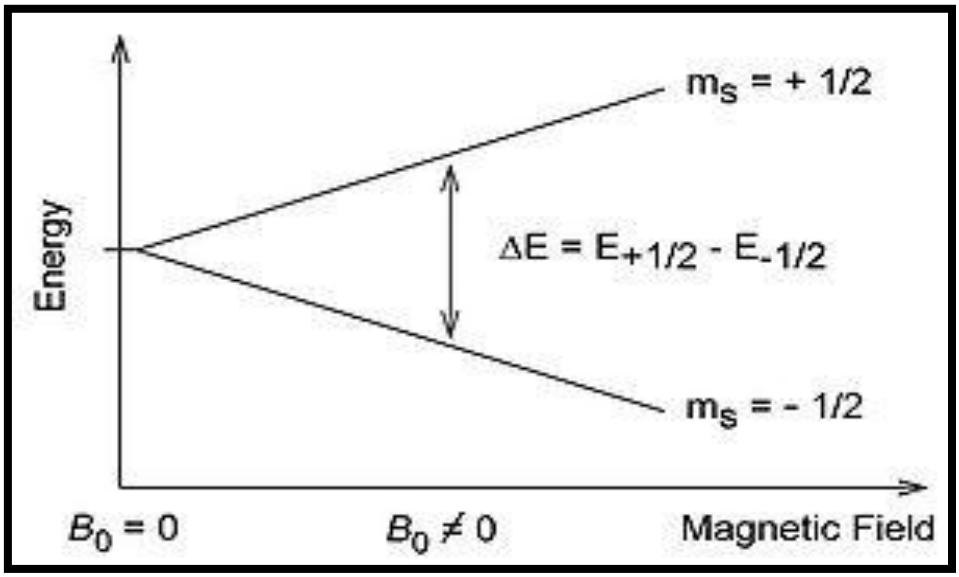

Figure 2.6. Splitting of energy level

The parallel alignment corresponds to the lower energy state, and the separation between it and the upper state is $\Delta E = g_e \mu_B B_0$, where g_e is the electron's so-called Lande g-factor and μ_B isthe Bohr magneton. This equation implies that the splitting of the energy levels is directly proportional to the magnetic field's strength, as shown in the Fig.2.6 [37]. An unpaired electron can move between the two energy levels by either absorbing or emitting electromagnetic radiation of energy $\varepsilon = h\nu$ such that the resonance condition, $\varepsilon = \Delta E$, is obeyed. Substituting in $\varepsilon = h$ and is $\Delta E = g_e \mu_B B_0$, leads to the fundamental equation $h\nu = ge\mu BB0$, . Experimentally, this equation permits a large combination of frequency and magnetic field values, but the great majority of EPR measurements are made with microwaves in the 9000 – 10000 MHz (9 – 10 GHz) region, with fields corresponding to about 3500 G [38][39]. The energy in principle of EPR spectra can be generated by either varying the photon

frequency incident on a sample while holding the magnetic field constant, or doing the reverse. In practice, it is usually the frequency which is kept fixed. A collection of paramagnetic centers, such as free radicals, is exposed to microwaves at a fixed frequency. By increasing an external magnetic field, the gap between the $m_s = +1/2$ and $m_s = -1/2$ energy states is widened until it matches of the microwaves [40], as represented by the double-arrow in the diagram above. At this point the unpaired electrons can move between their two spin states. Since there typically are more electrons in the lower state, due to the Maxwell-Boltzmann distribution there is a net absorption of energy, and it is this absorption which is monitored and converted into a spectrum[41][42].

EXPERIMENTAL TECHNIQUES

The schematic diagram of an EPR spectrometer is shown in Figure 2.7. The basic features of a spectrometer are:

1. A large electromagnet and its associated power supply
2. Source of microwave radiation-a klystron or a gunn diode
3. A sample cell (resonant cavity)
4. A detection system
5. A recorded or oscilloscope

A uniform magnetic field is generated by a powerful electromagnet with a Hall effect device modulation coils, located on either side of the resonant cavity to modulate the magnetic field.

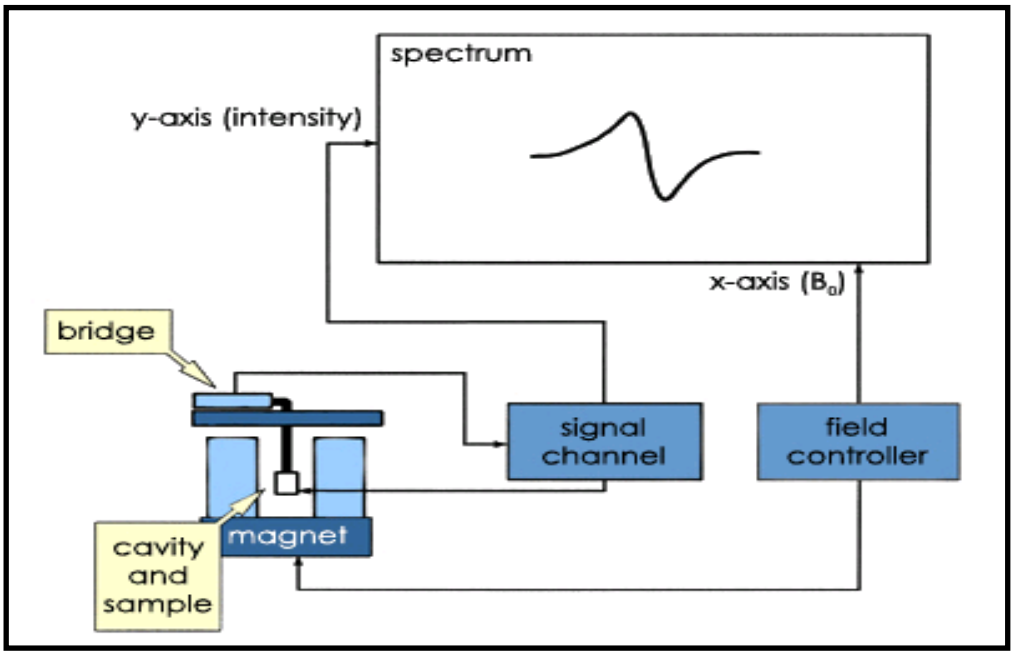

Figure 2.7 Block diagram of a typical X-band EPR spectrometer[22]

The source of microwave radiation may be either a klystron (vacuum tube) or gun diode (a solid state device) either of which provides a monochromatic, coherent source of electromagnetic radiation. Commonly the spectrometers operate in the X-bands frequency region corresponding to 9.36GHz. The source frequency can be swept either side of the center frequency by ± 100MHz for the purpose of tuning the microwave circuit and cavity.

The radiation is transmitted into the sample cell by means of a wave-guide, which is a copper or brass tubing. The sample cell is positioned between the poles of the electromagnet. The phase sensitive detector locked to the magnetic field modulation frequency carries out the electronic detection of the reflected microwave beam. The signal after amplification is either displayed on an oscilloscope or recorded on the chart paper. Instead of displaying the signal as the absorption curve, EPR signals, usually phase sensitive, are detected and represented as the first derivatives. The degeneracy of the electron spin states is

lifted when an unpaired electron is placed in a magnetic field, creating two spin states, $m_s = \pm ½$, where $m_s = - ½$, the lower energy

state, is aligned with the magnetic field. The spin state on the electron can flip when electromagnetic radiation is applied. In the case of electron spin transitions, this corresponds to radiation in the microwave range. The energy difference between the two spin

The radiation is transmitted into the sample cell by means of a wave-guide, which is a copper or brass tubing. The sample cell is positioned between the poles of the electromagnet. The phase sensitive detector locked to the magnetic field modulation frequency carries out the electronic detection of the reflected microwave beam. The signal after amplification is either displayed on an oscilloscope or recorded on the chart paper. Instead of displaying the signal as the absorption curve, EPR signals, usually phase sensitive, are detected and represented as the first derivatives. The degeneracy of the electron spin states is lifted when an unpaired electron is placed in a magnetic field, creating two spin states, $m_s = \pm ½$, where $m_s = - ½$, the lower energy state, is aligned with the magnetic field. The spin state on the electron can flip when electromagnetic radiation is applied. In the case of electron spin transitions, this corresponds to radiation in the microwave range. The energy difference between the two spin states is given by the equation

$$\Delta \mathbf{E} = \mathbf{E}_+ - \mathbf{E}_- = \mathbf{h}\nu = g\beta\mathbf{B}$$

where h is Planck's constant (6.626×10^{-34} J s^{-1}), v is the frequency of radiation, ß is the Bohr magneton (9.274×10^{-24} J T^{-1}), B is the strength of the magnetic field in Tesla, and g is known as the g-factor. The g-factor is a unit less measurement of the intrinsic magnetic moment of the electron, and its value for a free electron is 2.0023. The value of g can vary, however, and can be calculated by rearrangement of the above equation

$$g = \mathbf{h}\nu / \beta\mathbf{B}$$

using the magnetic field and the frequency of the spectrometer. Since h, *v*, and *ß* should not change during an experiment, g values decrease as B increases. The concept of g can be roughly equated to that of chemical shift.

2.3 TRANSMISSION ELECTRON MICROSCOPE

A transmission electron microscope (TEM), Joel make model JEM-200CX has been used to study the particle size of manganese zinc ferrite nanoparticle. It has a fully automated vacuum system. The state of the art electronic circuits, logical and compact design facilitate both operation and maintenance. For example, start up shut down and photography can be executed by a simple push button operation. Magnification and camera length can be directly readout regardless of any change in the accelerating voltage and recorded together with the film number on the film. Moreover the microscope provides very stable and excellent images at low to high magnification and a variety of diffraction patterns instantly. The available attachments can permit the specimen to be heated, cooled, tilted in-situ and also enable various signals from the specimen to be observed. The column of the microscope consists of an electron gun, two-stage condenser lens, an interlocking two-stage beam deflector, specimen chamber, and the image forming system, which is normally composed of an objective lens, two-stage intermediate lens and projector lens. Viewing chamber and camera chamber are also the parts of the column. The specimen chamber has a side entry stage. The specimen exchange device contains an airlock mechanism so that the specimen can be exchanged without breaking the column vacuum. The specimen holder has a capacity of holding two specimens. The specimen movement range in X and Y directions are ±1mm while along Z direction it is ± 0.5mm.The specimen can be tilted by an angle of ± 30^{o} (X-tilt). The viewing chamber consists of a viewing window to see image of the specimen formed on the fluorescent screen. A binocular with a clear field of view is also installed with it to see the ten times enlarged image and also for image focusing purposes. The approximate size of an individual particle in the image of the specimen on the photographic screen can also be estimated with the help of small scale provided on the photographic screen. This instrument has a fully automatic camera complete with a data-recording device and its specially

designed automatic exposure mechanism ensures optimum exposure. Since this camera is equipped with an air lock mechanism, rapid film exchange can be executed without breaking the vacuum of the column. The camera chamber has films loading capacity up to 50. The cut films having size 65mm X 90mm, supplied by Eastman Kodak Company U.S.A. were used for recording purpose

.

2.3.1 PRINCIPLE OF TRANSMISSION ELECTRON MICROSCOPE

The transmission electron microscope is used as one of the technique for structural characterization of the material. In TEM, the electron beam, which is almost parallel, is scattered by the specimen. In the case of crystalline materials this scattering takes form of one or two Bragg diffracted beams traveling at small angles (1 or 2 degree) with the incident beam. This diffracted are focused to form an electron diffraction pattern in its back focal plane and the image of the object at the focal plane of the first intermediate lens, which is magnified by the intermediate lenses and projected on the screen by the projector lens.

Fig. 2.8 Photograph of Transmission Electron Microscope

The TEM is an evacuated metal cylinder (the column) about 2 meters high with the source of illumination, a tungsten filament as the cathode, at the top. If the filament is heated at the high voltage between 40,000 to 100,000 volts is passed between it and the anode, the filament will emit electrons. These negatively charged electrons are accelerated to an anode (positive charge) placed just below the filament, some of which pass through a tiny hole in the anode, to form an electron beam which passes down the column. The speed at which they are accelerated to the anode depends on the amount of accelerating voltage present. Electro-magnets, placed at intervals down the column, focus the electrons, mimicking the glass lenses on the light microscope. The double condenser lenses focus the electron beam onto the specimen which is claimed into the removable specimen stage, usually on a specimen grid. As the electron beam passes through the specimen, some electrons are scattered whilst the remainder are focused by the objective lens either onto a phosphorescent screen or photographic film to form an image. Unfocused electrons are clocked out by the objective aperture, resulting in an enhancement of the image contract. The contract of the image can be increased by reducing the size of this aperture. The remaining lenses on the TEM are the intermediate lens is used to control magnification. The projector lens corresponds to the ocular lens of light microscope and forms a real image on the fluorescent screen at the base of the microscope column.

2.3.2 THEORY

Transmission electron microscopy can be used to examine particles that are too small for investigation with optical microscopes. TEM provides a powerful method for determining particle shapes as well as their size and degree of agglomeration. It uses the electrons the same way that optical microscopes use light (photons); the particles under investigation in an electron beam absorb and scatter electrons to produce a two-dimensional image. In TEM, electrons are generated by thermionic emission from a heated tungsten filament and are focused by magnetic lenses, which serve the same function as optical lenses. The interior of an electron microscope must be under high vacuum (less than 10^{-7}atm) to prevent scattering of the electron beam by air molecules. The TEM was the first

type of electron microscope to be developed and is patterned exactly on the light transmission microscope except that a focused beam of electrons is used instead of light to "see through" the specimen. It was developed by Max Knoll and Ernst Ruska in Germany in 1931.

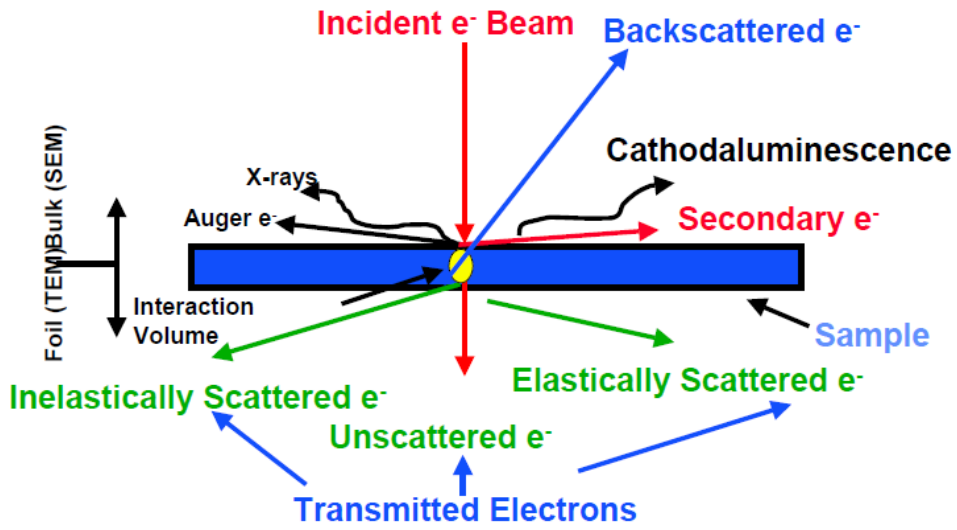

Figure 2.9 : signal generation due to interaction of sample and radiation

THE KIND OF INFORMATION THAT A TEM YIELDS ARE

MORPHOLOGY

The size, shape and arrangement of the particles which make up the specimen can be measured very well. The resolution can reach on the scale of atomic diameters.

Crystallographic Information

The arrangement of atoms in the specimen and their degree of order, detection of atomic-scale defects in areas a few nanometers in diameter

Compositional Information (if so equipped)

The elements and compounds the sample is composed of and their relative ratios, in areas a few nanometers in diameter.

WORKING PRINCIPLE

The schematic of the basic process is shown in figure. The accelerated electrons (from 100KeV to 400KeV) from the tungsten filaments are projected on thin specimen by means of condenser lenses system. The beam strikes the specimen and parts of it are transmitted. This transmitted portion is focused by the objective lens in to an image Optional Objective and Selected Area metal apertures can restrict the beam; the Objective aperture enhancing contrast by blocking out high-angle diffracted electrons, the Selected Area aperture enabling the user to examine the periodic diffraction of electrons by ordered arrangements of atoms in the sample. The image is passed down the column through the intermediate and projector lenses, being enlarged all the way the image strikes the phosphor image screen and light is generated, allowing the user to see the image. The high resolution of TEM is due to small effective wavelength of electrons, given by De Broglie relationship:

$$\lambda = h / (2mqV)^{1/2}$$

where h is Planck's constant, m and q are electron mass and charge and V is potential difference through which electrons are accelerated. The higher is the operating voltage, the greater the resolution.

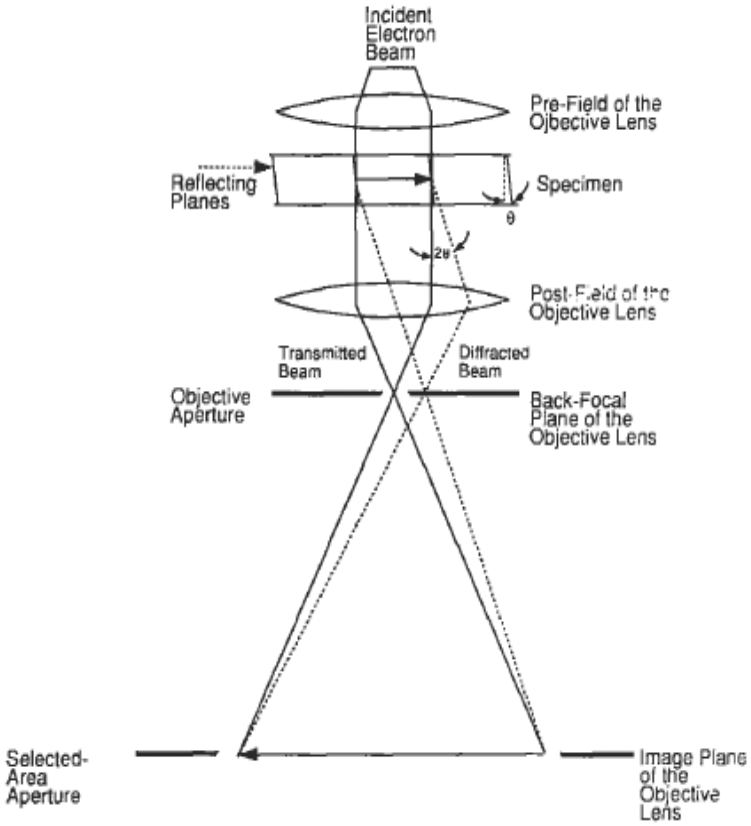

Figure 2.10 : Optical path area of beam during tem operation.

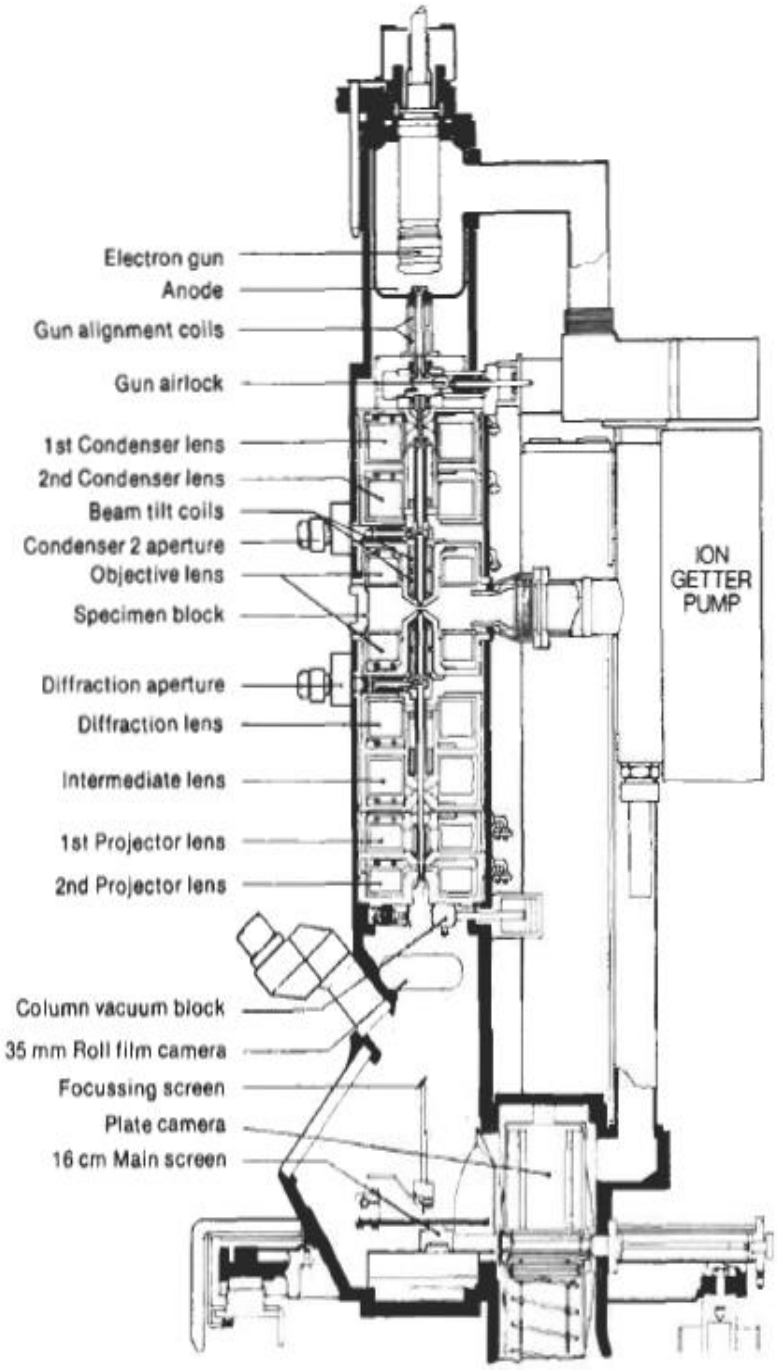

Figure 2.11 : Detailed diagram of TEM instrument.

Limitations of TEM

Sample preparation

Sample preparation is one of the primary tasks in case of TEM characterization. For sample preparation, typically very fine carbon-coated copper meshes 3 mm in diameter (here called TEM grids) are used. To form a high-contrast picture, their carbon film has to be sufficiently thin compared to the particles, causing only slight attenuation in comparison with the particles, which extensively scatter and absorb the electron beam. Very small amounts of powder are placed on the TEM grids by dipping the grid in the powder, preparing a dilute solution with an evaporating fluid (e.g. acetone). A rule of thumb for coverage of the TEM grid is that about 10% or less should be covered with particles. TEM requires a sample thin enough to be electron transparent, which makes analysis a relatively time consuming process with a low throughput of samples. The structure of the sample may also be changed during the preparation process. Also the field of view is relatively small, raising the possibility that the region analyzed may not be characteristic of the whole sample. There is potential that the sample may be damaged by the electron beam, particularly in the case of biological materials.

3. RESULT AND DISCUSSIOIN

3.1 STRUCTURAL CHARACTERIZATIOsN

The structural analysis of $Mn_xZn_{1-x}Fe_2O_4$ (x= 0.1,0.3,0.5) samples was done by powder X-ray diffraction technique at 40kV, 30 mA using Cu K_α radiation. Fig. (3.1, 3.2, 3.3) shows the powder X-ray diffraction patterns for as-synthesized and annealed (573°K, 773°K, 973°K, 1173°K , 1373°K) samples with various manganese and zinc compositions.

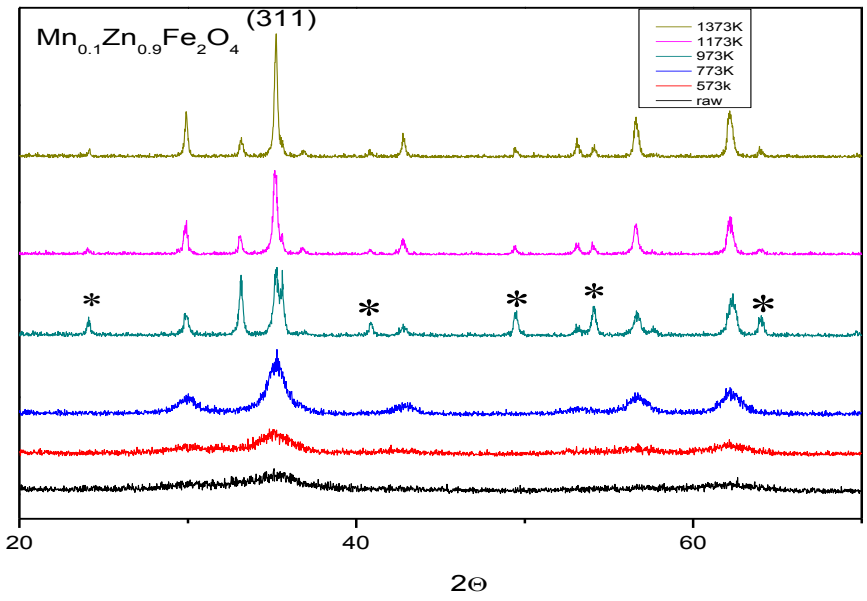

Figure. 3.1 X-ray diffraction pattern of $Mn_{0.1}Zn_{0.9}Fe_2O_4$ at different annealing temperature

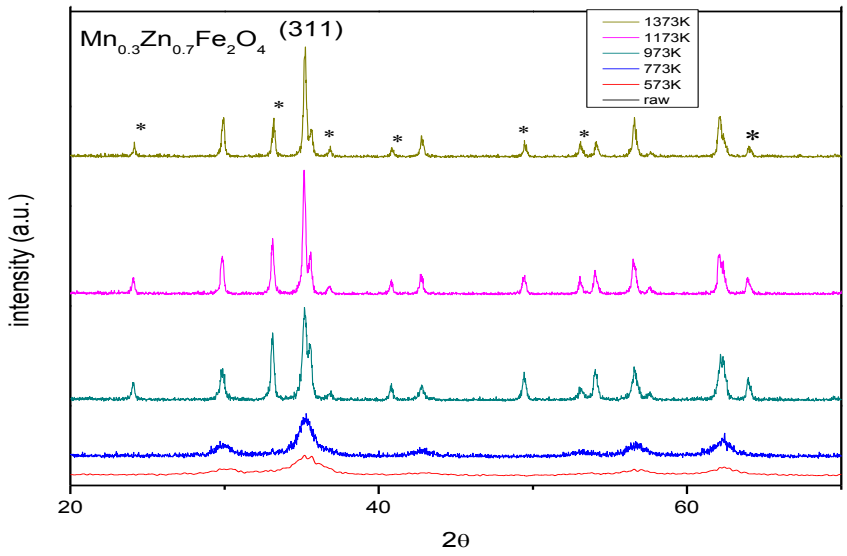

figure. 3.2 X-Ray pattern of $Mn_{0.3}Zn_{0.7}Fe_2O_4$ at different annealing temperature

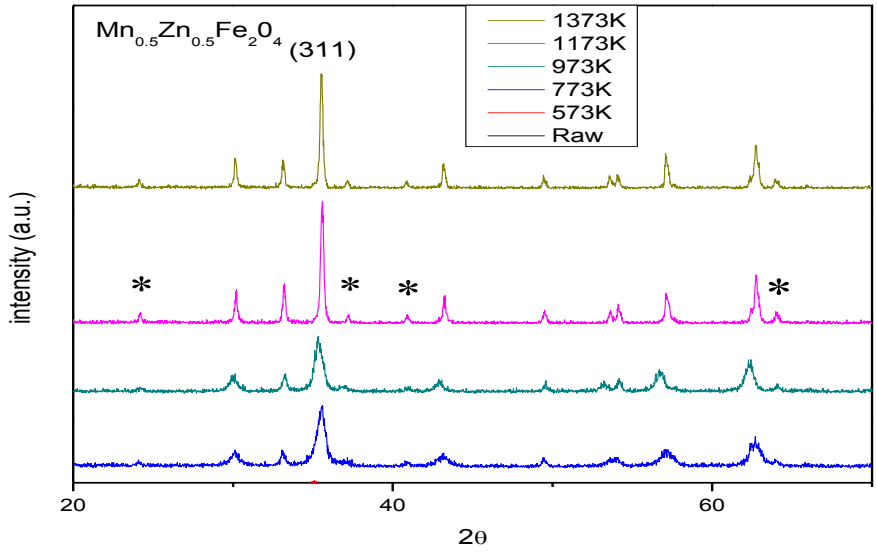

Figure. 3.3 X-Ray pattern of $Mn_{0.5}Zn_{0.5}Fe_2O_4$ at different annealing temperature

X-ray diffraction pattern of as-synthesized particles shows broad peaks indicating ultra fine nature and small crystallite size of the particles. On annealing of samples the X-ray diffraction patterns show an improvement in the sharpness and intensity of the peaks. The XRD patterns were analyzed by using JADE software. Table 1, 2, 3 gives the X-ray analysis of these samples.

The '*d*' values and intensities of observed diffraction peaks match with the single crystalline spinel form of the magnese zinc ferrite (JCPDS Card No. 019-0692). The lattice parameters along with the crystallite size were calculated for all the compositions and are listed in Tables 2 for $Mn_{0.1}Zn_{0.9}Fe_2O_4$, table 3 for $Mn_{0.3}Zn_{0.7}Fe_2O_4$and 4 for $Mn_{0.5}Zn_{0.5}Fe_2O_4$. A Scherrer Formulae is used in x-ray diffraction and crystallography to correlate the size of sub-micrometre particles, or crystallites, in a solid to the broadening of a peak in a diffraction pattern. In the Scherrer equation,

$$\tau = \frac{K\lambda}{\beta \cos\theta}$$

Where τ is the mean crystallite dimension, K is the shape factor, λ is the x-ray wavelength, typically 1.54 Å, β is the line broadening at half the maximum intensity (FWHM) in radians, and θ is the Bragg angle. The dimensionless shape factor has a typical value of about 0.9, but varies with the actual shape of the crystallite.

Table 2. Crystallite size and lattice parameter of $Mn_{0.1}Zn_{0.9}Fe_2O_4$ with different annealing temperature

Composition	Annealing temperature	Crystallite size (nm)	Lattice parameter (A°)
$Mn_{0.1}Zn_{0.9}Fe_2O_4$	Raw	1.44	8.338
$Mn_{0.1}Zn_{0.9}Fe_2O_4$	300	3.37	8.413
$Mn_{0.1}Zn_{0.9}Fe_2O_4$	500	6.75	8.425
$Mn_{0.1}Zn_{0.9}Fe_2O_4$	700	12.75	8.439
$Mn_{0.1}Zn_{0.9}Fe_2O_4$	900	26.27	8.458
$Mn_{0.1}Zn_{0.9}Fe_2O_4$	1100	35.40	8.468

3. Crystallite size and lattice parameter of $Mn_{0.3}Zn_{0.7}Fe_2O_4$ with different annealing temperature

Composition	Annealing temperature	Crystallite size (nm)	Lattice parameter (A°)
$Mn_{0.3}Zn_{0.7}Fe_2O_4$	Raw	2.19	8.411
$Mn_{0.3}Zn_{0.7}Fe_2O_4$	300	3.88	8.426
$Mn_{0.3}Zn_{0.7}Fe_2O_4$	500	6.43	8.441
$Mn_{0.3}Zn_{0.7}Fe_2O_4$	700	13.97	8.453
$Mn_{0.3}Zn_{0.7}Fe_2O_4$	900	32.60	8.458
$Mn_{0.3}Zn_{0.7}Fe_2O_4$	1100	33.20	8.483

Table 4. Crystallite size and lattice parameter of $Mn_{0.5}Zn_{0.5}Fe_2O_4$ with different annealing temperature.

Composition	Annealing temperature	Crystallite size (nm)	Lattice parameter (A°)
$Mn_{0.5}Zn_{0.5}Fe_2O_4$	Raw	3.27	8.357
$Mn_{0.5}Zn_{0.5}Fe_2O_4$	300	8.60	8.375
$Mn_{0.5}Zn_{0.5}Fe_2O_4$	500	12.14	8.416
$Mn_{0.5}Zn_{0.5}Fe_2O_4$	700	13.06	8.444
$Mn_{0.5}Zn_{0.5}Fe_2O_4$	900	33.99	8.449
$Mn_{0.5}Zn_{0.5}Fe_2O_4$	1100	36.37	8.472

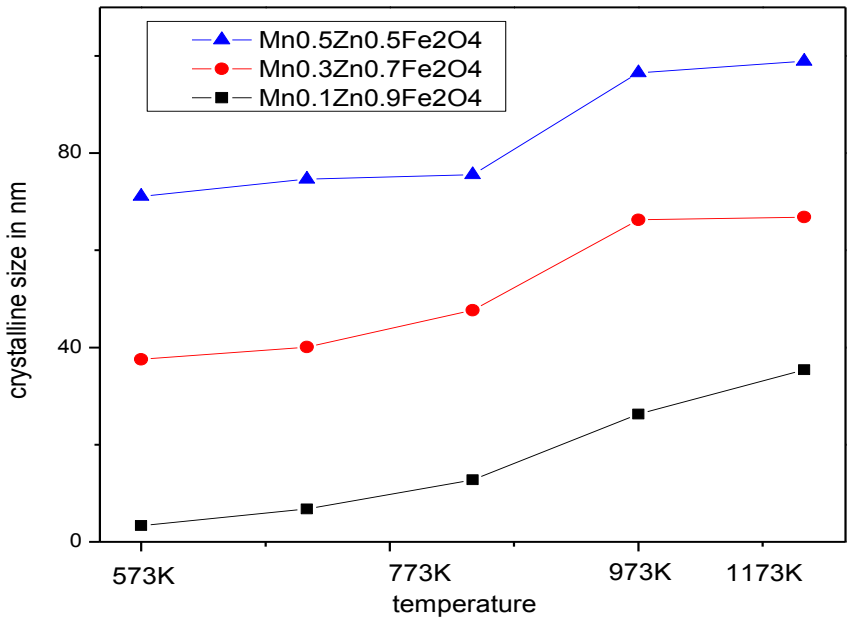

Figure 3.4 Variation of crystallite size with temperature for $Mn_xZn_{1-X}Fe_2O_4$ (X=0.1,0.3,0.5)

XRD RESULTS

The XRD pattern of $Mn_xZn_{1-x}Fe_2O_4$ for x = 0.1, 0.3, 0.5 samples at different annealing temperature is shown in fig 3.2, 3.3, 3.4. All peaks observed in the spectra corresponds to FCC spinel structure. The crystallite size of all the samples were calculated using Scherrer's formula table 2, 3, 4 gives the value of crystallite size and lattice parameter. In Scherrer's formula where the full width half maximum of (311) plane is considered into calculation, from table 2, 3, 4, the particle size increases with increasing Mn concentration. From figure 2.1 we can see that the particle size first increases slowly nearly up to 973 K then changes rapidly up to 1173 and then remains nearly constant. The XRD pattern shows that in raw material there are very few and broad peaks are present but when the annealing temperature increases then the peaks becomes more sharp and more peaks generate.

3.2 ELECTRON PARAMAGNETIC RESONANCE

Electron Paramagnetic Resonance is very sensitive technique for the characterization of magnetic properties and the spin dynamics in solids. CW X-band EPR spectra are recorded by putting a sample into a microwave irradiation field of constant frequency ν and sweeping the external magnetic field B0 until the resonance condition is fulfilled. The line and the shape of the resonant signal give information about the magnetic and electronic state. This work describes the systematic studies on EPR parameter like peak-to-peak line width (ΔH_{PP}), spin concentration (Ns) of sample. The EPR spectra of as synthesized samples were recorded by scanning the magnetic induction at constant microwave frequency(i.e. 9.36 GHz in X-band EPR spectrometer) in the 4000 ± 4000G scan region at 1.25×10 gain and 1×1 modulation at room temperature is shown in figure. All spectra were analyzed using Lorentzian distribution to obtained various parameter such as ΔH_{pp} , g-value and Ns [40,41,42] these values are listed in Table-5.The spectra of these samples show a single broad

signal with a very weak hump signal, indicating the presence of isolated Fe^{3+},Mn^{2+}, Zn^{2+} ions of g-value of about 2.04. The broadness of the EPR resonance signal is due to random orientation of ferromagnetic particles in samples, which scatter in directions of anisotropic field of nanoparticles [37, 38, 39].

Table 5: $Mn_{0.1}Zn_{0.9}Fe_2O_4$ samples at different annealing temperature

$Mn_{0.1}Zn_{0.9}Fe_2O_4$ Raw at different annealing temperature	**ΔH_{PP} (Gauss)**	**g-value**	**Signal intensity**	**(spin/gm) N_S**	**relaxation time (T2)**
Raw	261.7	1.99816	3.135×10^{9}	$2.798x10^{15}$	1.25×10^{-10}
(573K)	209.3	1.99892	3.505×10^{9}	$3.128x10^{15}$	1.56×10^{-10}
(773K)	276.4	1.99870	7.145×10^{8}	$6.377x10^{14}$	1.18×10^{-10}
(973K)	560.7	2.01680	1.043×10^{9}	$9.308x10^{14}$	5.81×10^{-10}
(1173K)	438.3	2.09712	2.408×10^{9}	2.149×10^{15}	7.16×10-11

Table 6: $Mn_{0.3}Zn_{0.7}Fe_2O_4$ samples at different annealing temperature

$Mn_{0.1}Zn_{0.9}Fe_2O_4$ Raw at different annealing temperature	ΔH_{PP} (Gauss)	g-value	Signal intensity	(spin/gm) N_S	relaxation time (T2)
Raw	-	-	-	-	-
(573K)	244.8	1.99774	6.469×10^{8}	5.773×10^{14}	4.957×10^{-11}
(773K)	442.3	2.03957	6.581×10^{9}	5.873×10^{15}	7.273×10^{-11}
(973K)	647.6	2.04393	2.891×10^{8}	2.580×10^{14}	4.957×10^{-11}
(1173K)	892.4	2.10120	7.046×10^{8}	6.288×10^{14}	3.498×10^{-11}
1373K	931.9	2.14622	7.694×10^{9}	6.866×10^{15}	3.280×10^{-11}

Table 7 $Mn_{0.5}Zn_{0.5}Fe_2O_4$ samples at different annealing temperature

$Mn_{0.5}Zn_{0.5}Fe_2O_4$ Raw at different annealing temperature	ΔH_{PP} (Gauss)	g-value	Signal intensity	(spin/gm) N_S	relaxation time (T2)
Raw	355.4	2.00351	2.011×10^{9}	1.794×10^{15}	9.215×10^{-11}
(573K)	236.9	4.72248	7.222×10^{8}	6.445×10^{14}	5.861×10^{-11}
(773K)	363.5	3.28879	1.411×10^{9}	1.259×10^{15}	5.488×10^{-11}
(973K)	608.1	2.08979	2.803×10^{9}	2.501×10^{15}	5.163×10^{-11}
(1173K)	331.7	1.99342	3.945×10^{8}	3.520×10^{14}	9.923×10^{-11}
(1373K)	252.7	2.03093	3.254×10^{8}	2.904×10^{14}	1.278×10^{-10}

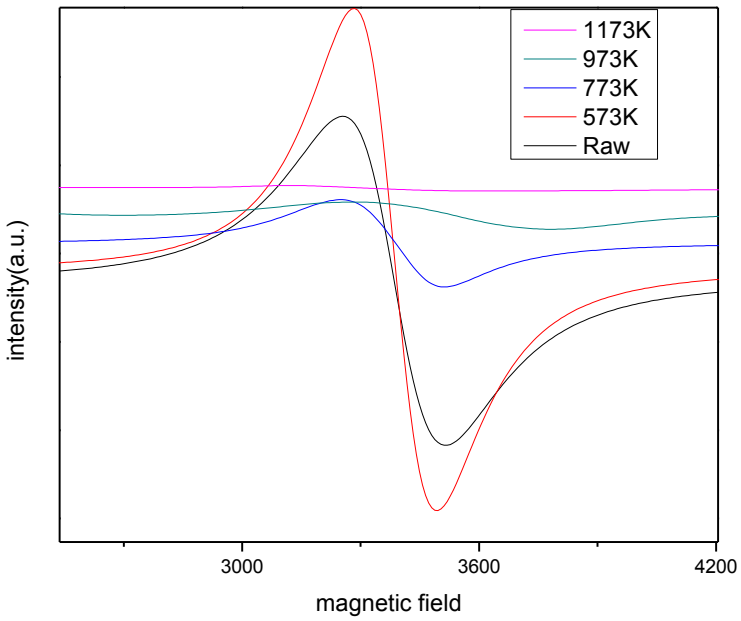

Fig 3.5 EPR curve for $Mn_{0.1}Zn_{0.9}Fe_2O_4$ annealed at different temperature

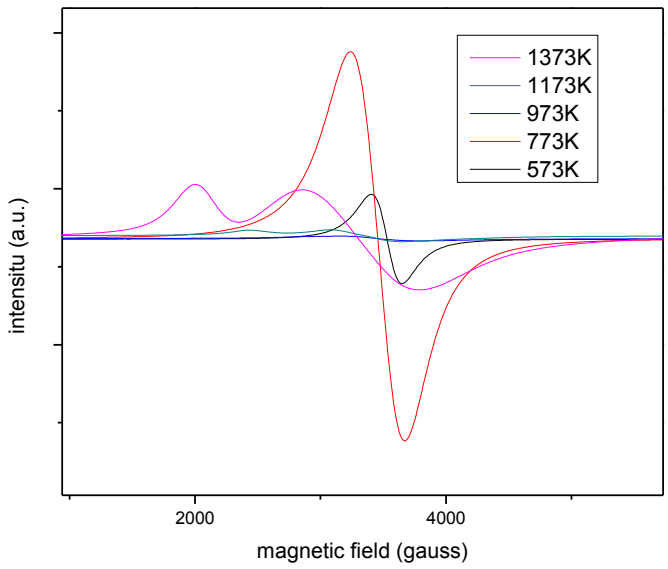

Fig 3.6 EPR curve for $Mn_{0.3}Zn_{0.7}Fe_2O_4$ annealed at different temperature

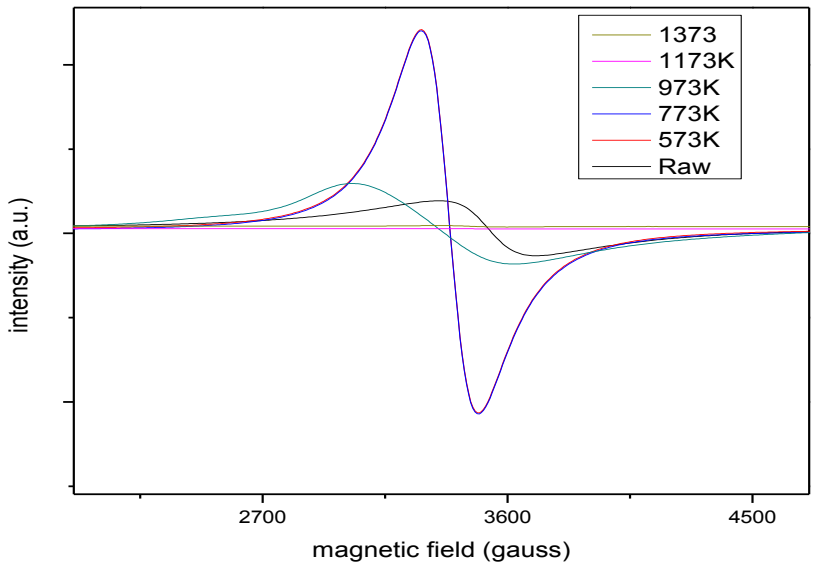

Fig 3.7 EPR curve for $Mn_{0.5}Zn_{0.5}Fe_2O_4$ annealed at different temperature

The g-value, which is a constant of proportionality between the frequency and the field, is a function of the molecular motion, the paramagnetic properties and the symmetry of ions [40,41,42]. The value of g is calculated by the relation

$$g = h\nu / \beta H$$

where, h is a Plank constant, ν is the microwave frequency, β is Bohr magneton and H is the magnetic field at the resonance.

EPR RESULT

Electron paramagnetic resonance (EPR) spectroscopy, also known as electron spin resonance (ESR) , is the most powerful technique for studying unpaired electrons. From table 5, 6, 7 the g value of raw material increases with manganese concentration. Table 5, 6, 7 also shows the

spin concentration and relaxation time the spin concentration decreases with increasing Mn concentration and relaxation time also decreases. Tables 5, 6, 7 also shows the the g value, spin concentration and relaxation time at different annealing temperature. Fig 3.5, 3.6, 3.7 shows the EPR spactra at different annealing temperature.

3.3 TRANSMISSION ELECTRON MICROSCOPY

The transmission electron microscopic is one of the important technique to investigate nano- crystalline material for shape and the size determination and electron differaction for structural information. In , TEM the electron beam is scattered by the specimen, scattering takes from of one or two Bragg differected beams travelling in small angle (1°or 2°) with the incident beam. These diffracted beams are focused to form an electron diffraction pattern and the image of the object at the focal plane of the first immediate lens which is magnified by the intermediate lens and projector lenses. Thus transmission electron microscope gives shape and size distribution of the doveloped nano particles.

The synthesized nano-particles are studied by transmission electron microscope for particle size determination. For measuring the size of nano-particles a drop of the nanoparticle dispersion liquid was put on the TEM grid and the solvent (aceton/octane /hexane) was allowed to dry in air. Copper grid with a carbon film deposited on a formvar backing, were used for preparing the TEM samples. The solvent is which also hydrophobic spread out on the grid instead of staying agglomerated in the form of a small drop as formvar is more hydrophobic than carbon and the nanoparticles spread over the carbon grid. For TEM imaging of the nanoparticles magnified shadow of the particles was recorded. Bright field images

were captured on to a negative, which were then developed and latter scanned as a digital copy.

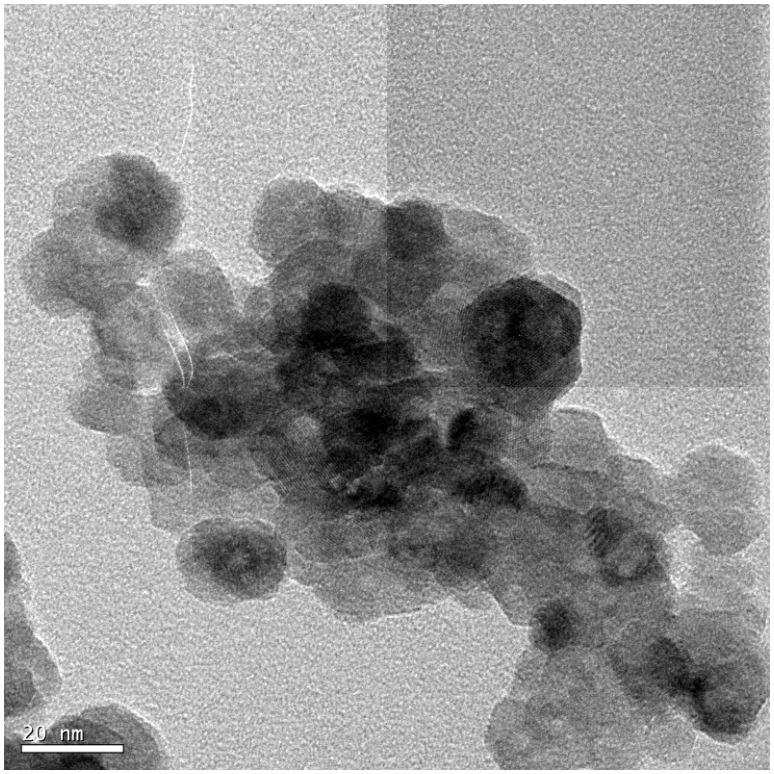

Fig 3.8 Tem photograph of $Mn_{0.1}Zn_{0.9}Fe_2O_4$ raw particles

TEM results of $Mn_XZn_{1-X}Fe_2O_4$ particles

Figure 3.8 shows the TEM micrograph recorded for $Mn_{0.1}Zn_{0.9}Fe_2O_4$ raw particles. From the TEM image it can be concluded that the doveloped particles are of very small size lying in the nano range and have homogenous size distribution and shape symmetry. Almost, all the particles are in spherical in shape and are of ~25 nm in si

Chapter 4

CONCLUSION

The main focus of the present work is to synthesize nano magnetic particles of $Mn_xZn_{1-x}Fe_2O_4$ based ferrites suitable for application .The compound synthesized are $Mn_{0.1}Zn_{0.9}Fe_2O_4$, $Mn_{0.3}Zn_{0.7}Fe_2O_4$ and $Mn_{0.5}Zn_{0.5}Fe_2O_4$ and to make use of them for the preparation of ferrofluids. The effect on the physical properties is investigated. The effect of the annealing on the properties of the fine particles is also carried out. These fine particles were prepared by using the chemical co-precipitation rout.

The fine particles are characterized by X-ray diffraction technique ,EPR spectroscopy, TEM transmission electron microscopy, Structural analysis like crystallite size, lattice parameter and strain estimation is determined by powder X-ray diffraction technique and variation in physical properties has been investigated. The increase on crystallite size, and lattice parameter of the particles is compare to material has been observed. From X-Ray diffractometer we observed that the raw material has spinel structure and when the annealing temperature increases then the peaks gets sharper it means the crystallite size increases. Effect of annealing temperature observed and found that when the temperature increases then the intensity and d values of entire observed diffraction peaks for the sample annealed at 573k, and 773K, perfectly match with the single crystalline phase of spinel structure form $Mn_xZn_{1-x}Fe_2O_4$. on further increasing the annealing temperatures 973K, 1173K, 1373K, material does not remain in single phase and part of the material gets converted into hematite phase which is nearly non magnetic and reduces the usability of the material**.** ***It is due to the reason that at higher temperature the thermal stability of the $Mn_xZn_{1-x}Fe_2O_4$ material reduces and the absorption of oxygen leads to form an extra phase of hematite.***

Magnetization characterization is done with EPR spectroscopy. EPR spactra of the synthesized ferrite materials were recorded on Q- and X- band WIN EPR spectrometer (Bruker biospin make) at ambient temperature in order to study the effect of magnetic field on the energy level splitting in these ferrite particles. The instrument calculated the g value and ΔH_{PP} values and intensity with the help of these values we found spin

concentration and relaxation time. Pattern and values shows that when the annealing temperature increases then the pattern gets in flat shape it means the spin are more confine and there is not absorption of microwave concentration increases so the spin concentration decreases and when annealing temperature increases then the spin concentration decreases because hematite phase present there so the magnetization decreases. The surface morphology of these fine particles is characterized by using transmission electron microscope. TEM micrograph recorded for $Mn_{0.1}Zn_{0.9}Fe_2O_4$ raw particles. From the TEM image it can be concluded that the doveloped particles are of very small size lying in the nano range and have homogenous size distribution and shape symmetry. Almost, all the particles are in spherical in shape and are of ~25 nm in size.

REFERENCES

1. B.D.Cullity, Introduction to magnetic materials, Page 88.
2. B.D.Cullity, Introduction to magnetic materials, Page 110.
3. R.K.Puri, V.K.Babbar, Solid State Physics &Electronics, Chapter page 236 , S.Chand & Company LTD.,1997
4. B.D.Cullity, Introduction to magnetic materials, Page 156.
5. R.K.Puri, V.K.Babbar, Solid State Physics &Electronics, Chapter page 250 , S.Chand & Company LTD.,1997
6. E.C. Stoner, E.P. Wohlfarth, A mechanism of magnetic hysteresis in heterogeneous alloys, Philos. Trans. R. Soc. A240 (1948) 599–642..
7. B.D.Cullity, Introduction to magnetic materials, Page 248,284
8. Williams F. Smith, Javad Hashemi, Foundations of *Materials Science and Engineering*, fourth Edit. chapter 16, page 888, Mc Graw-Hill 2006.
9. R.K.Puri, V.K.Babbar, Solid State Physics &Electronics, S.Chand & Company LTD.,1997
10. S.Chickazumi and S.H. Charap, "Physics of Magnetism" , Krieger Malabar (1978).
11. William H.Von Aulock, "Hand Book of Microwave Ferrite Materials" , Acadmic Press, New York London (1965).
12. B.H. Sohn, R.E. Cohen, Processible optically transparent block copolymer films containing superparamagnetic iron oxide nanoclusters, Chem. Mater. 9 (1997) 264–269.
13. Y.I. Kim, D. Kim, C.S. Lee, Synthesis and characterization of CoFe2O4magnetic nano particles prepared by temperature-controlled coprecipitation method, Physica B 337 (2003) 4251.

14. C. Caizer, M. Popovici, C. Savii, Spherical (ZndNi1-dFe2O4) nanoparti- cles in an amorphous (SiO2)1-γγ matrix, prepared with the sol–gel method, Acta Mater. 51 (2003) 3607–3616.

15. D.K. Kim, Y. Zhang, W. Voit, K.V. Rao, M. Muhammed, Synthesis and characterization of surfactant-coated superparamagnetic monodispersed iron oxide nanoparticles, J. Magn. Magn. Mater. 225 (2001) 30–36.

16. J.A.L.Perez,M.A.L.Quintela,J.Mira,J.Rivas,S.W.Charles,Advancesin the preparation of magnetic nanoparticles by the microemulsion method, J. Phys. Chem. B 101 (1997) 8045–8047. [6] Q. Chen, Z.J. Zhang, Size-dependent superparamagnetic properties of MgFe2O spinel ferrite nanocrystallites, Appl. Phys. Lett. 73 (1998) 3156–3158.

17. Z.X. Tang, C.M. Sorensen, K.J. Klabunde, G.C. Hadjipanayis, Preparation of Mn ferrite fine particles from aqueous solution, J. Colloid Interface Sci. 146 (1991) 38–46.

18. C.T. Seip, E.E. Carpenter, C.J. O'Connor, V.T. John, S. Li, Magnetic prop- erties of a series of ferrite nanoparticles synthesized in reverse micelles, IEEE Trans. Magn. 34 (1998) 1111–1113.

19. J.F. Hochepied, P. Bonville, M.P. Pileni, Nonstoichiometric zinc ferrite nanocrystals: syntheses and unusual magnetic properties, J. Phys. Chem. B 104 (2000) 905–912.

20. C. Liu, B. Zou, A.J. Rondinone, Z.J. Zhang, Reverse micelle synthesis and characterization of superparamagnetic MnFe2Ospinel ferrite nanocrys- tallites, J. Phys. Chem. B 104(2000)1141–1145.

21. H. Gleiter, Prog. Mater. Sci. **33** (1989) 223.

22. R. W. Siegel, Nanostructured Mater. **4** (1994) 121.

23. Chin-Yih. Hong, I. J. Jang, H. E. Horng, C. J. Hsu, Y. D. Yao, and H. C. Yang, J. Appl. Phys. **81** (1997) 4275.

24. M. Grätzel, Nature **414** (2001) 338.

25. H. Gleiter, Prog. Mater. Sci. 33 (1989) 223.

26. T. Mütschele and R. Kirchheim, Scripta Metall. 21 (1987) 1101

27. V.G.Bashtovoy, B.M.Berkovsky and A.N.Vislovich, Introduction to magnetic fluids. Washington (1988)

28. R.K.Puri, V.K.Babbar, Solid State Physics &Electronics, S.Chand & Company LTD.,1997

29. N. A. Brusentsov, L. V. Nikitin, T. N. Brusentsova, A. A. Kuznetsov, F. S. Bayburtskiy, L. I. Shumakov, and N. Y. Jurchenko "Magnetic fluid hyperthermia of the mouse experimental tumor", Journal of Magnetism and Magnetic Materials, 252, 378 (2002)

30. V. Bashtovoi, "Static of Magnetic Fluids",

31. K. Raj, "Magnetic Fluids and Devices: a Commercial Survey"

32. H. Gleiter, Prog. Mater. Sci. **33** (1989) 223.

33. R. W. Siegel, Nanostructured Mater. **4** (1994) 121.

34. Richard M. Bozorth, Ferromagnetism, first published 1951, reprinted 1993 by IEEE Press, New York.

35. Kip Thorne, Spacetime Warps and the Quantum: A Glimpse of the Future, ITP & CalTech, 1999

36. Electronic Materials Dr. Helmut Föll University of Kiel; Faculty Of Engineering.

37. Shriver, D. F.; Atkins, P. W.; Overton, T. L.; Rourke, J. P.; Weller, M. T.; Armstrong, F. A. "Inorganic Chemistry" W. H. Freeman, New York, pp. 168-190, 2006.

38. A. Goldman, Modern Ferrite Technology. New York: Van Nostrand Reinhold, 1990; N. Spaldin, Magnetic materials: Fundamentals and device applications Cambridge: Cambridge University press, 2003.

39. Kip Thorne, Spacetime Warps and the Quantum: A Glimpse of the Future, ITP & CalTech, 1

40. Odom, B.; Hanneke, D.; D'Urso, B.; and Gabrielse, G. (2006). "New Measurement of the Electron Magnetic Moment Using a One-Electron Quantum Cyclotron". *Phyical Review Letters* 97: 030801.

41. Electronic Materials Dr. Helmut Föll University of Kiel; Faculty of Engineering.

42. W.L. Bragg, "The Diffraction of Short Electromagnetic Waves by a Crystal",Proceedings of the Cambridge Philosophical Society, 17 (1913), 43–57.